# CHAPTER ONE

# INTRODUCTION

## 1.1 Introduction

Shell structures are three dimensional bodies with one dimension much smaller than the other two dimensions. The shell structure is typically found in nature as well as in classical architecture. The efficiency of shell structures is based on its curvature (single or double), which allows a multiplicity of alternative stress paths and gives the optimum form for transmission of many different load types. Various different types of steel/concrete shell structures have been used. Singly curved shells, for example, can be found in oil storage tanks, the central part of some pressure vessels, in storage structures such as silos, in industrial chimneys and in tall structures like lighting columns. The single curvature allows very simple construction process and is very efficient in resisting certain types of loads. In some cases, it is better to take advantage of double curvature. Double curved shells are used to build spherical gas reservoirs, concrete roofs, vehicles, water towers and hanging roofs. Based on thickness/span ratio shells can be classified as thin, moderately thick and thick.

Composite laminates are formed by stacking layers of different composite materials and/or fiber orientation. Composite laminates have their planar dimensions of one or two orders of magnitude larger than their thickness. Often laminates are used in applications that require axial and bending strengths. Therefore, composite laminates are treated as plate or shell elements. Practical examples of composite shells are: laminated buried pipes carrying gas or oil, concrete roofs and stiffened plates and shells.

Laminated shell structures are finding increasing interest in engineering applications. Consequently, efficient and robust computational tools are required for the analysis of such structural models. Direct analytical method of analysis of laminated shell structures is very tedious and sometimes impossible. Therefore the finite element method becomes a logical alternative. As a matter of fact, large amount of laminate finite elements have been developed and incorporated in most commercial codes for structural analysis such as **SAP** or **STAAD**.

In this research a robust stabilized finite element formulation for the analysis of laminated shell structures under large rotations and large displacements conditions is developed. The geometric nonlinear formulation is based on total Lagrangian approach and using both Green's strains and geometric strains. A comparison is made between results obtained by Green's strain formulation and geometric strain formulation. The elements are continuum degenerated-based shell elements and utilize the standard isoparametric formulations. Three purely displacement based elements have been developed having four, eight and nine nodes, respectively. Each element possesses five degrees of freedom per node, three displacements and two rotations.

Since elements used are displacement-based finite elements, problems of shear locking must be solved. This is done by using Mixed Interpolation Tensorial Components (MITC) techniques proposed by Bathe (1996) [6].

The significance of this research is emphasized by the importance of studying linear and nonlinear behavior of laminated shells subject to large rotations and large displacements with possibility of local buckling because such structures nowadays are widely constructed in Sudan in form of hall roofs, concrete roofs, pipe lines (gas and oil) and large water tanks.

The limitation of the formulation will be investigated thoroughly by performing parametric studies.

## 1.2 Objectives

The objectives of this research are:

1- To develop displacement finite elements suitable for the analysis of laminated shell structures.

2- To develop a robust geometrically nonlinear stabilized finite element formulation for modeling laminated shell structures under large rotations and large displacements.

3- To develop and implement a computer program based on the formulation in (2).

4- To test the program by analyzing a number of laminated shell structures and comparing results obtained with published results.

5- To compare results (stresses, strains and displacements) obtained when using Green's strains formulation with those obtained by using Geometric (engineering) strains formulation.

## 1.3 Methodology

The methodology of the present research is composed of four steps as follows:

Step 1: developing a geometric nonlinear finite element formulation for analysis of laminated shell structures and investigating the defects of the formulation e.g. locking.

Step 2: some techniques are proposed to overcome shortcomings associated with the development of the above mentioned formulations.

Step 3: developing FORTRAN computer program based on the formulation developed.

Step 4: implementing the program by analyzing some laminated shell structures and verifying the results obtained by comparison with known solutions.

## 1.4 Research Outlines

This research consists of seven chapters, the content of which can be summarized as follows:

**Chapter One** covers general introduction.

**Chapter Two** introduces literature review of laminated shell and their analysis using finite element.

**Chapter Three** presents a linear formulation for analysis of laminated shell structures.

**Chapter Four** presents nonlinear analysis of laminated shells.

**Chapter Five** describes the computer program developed.

**Chapter Six** contains application to numerical examples results discussion.

**Chapter Seven** presents the conclusions and recommendations drawn from this study.

# CHAPTER TWO

# LITERATURE REVIEW

## 2.1 Composites Materials

A Composite material in engineering is any material that has been physically assembled to form one single bulk without physical blending to form a homogeneous material. The resulting material would still has components identifiable as the constituent of the different materials. One of the advantages of composite materials is that two or more materials could be combined to take advantage of the good characteristics of each material.

Usually, composite materials consist of two separate components, namely the matrix and the filler. The matrix is the component that holds the filler together to form the bulk of the material. It usually consists of various epoxy type polymers but other materials may also be used. Metal matrix composite and thermoplastic matrix composite are some of the possibilities. The filler is the material that has been impregnated in the matrix to lend its advantage (usually strength) to the composite. The fillers can be any kind of material such as carbon fiber, glass bead, or ceramic.

Composite materials can be classified into four types according to the filler type as follows:

1. Particulate composite material
2. Short or long fiber composite material
3. Laminate composite material
4. Combination composite material

A Particulate composite material consist of the composite material in which the filler materials are roughly round. An example of this type of composite material would be the unreinforced concrete where the cement is the matrix and the sand serves as the filler. Lead particles in copper matrix are another example where both the matrix and the filler are metals.

Short fiber composites are composites in which the filler material has a length to diameter ratio less than one. Long fiber composites are generally taken to have a length to diameter ratio greater than 100. Fiber glass filler for boat panel is an example of short fiber composite. Carbon fiber is one of the filler material used in the long fiber type composites. Laminate is the type of composite that uses the filler material in the form of sheet instead of round particles or fibers. Formica countertop is a good example of this type of composite. The matrix material is usually phenolic type thermoset polymer. The filler could be any material from craft paper (Formica) to canvas (canvas phenolic) to glass (glass filled phenol).

Since the composites are non-homogeneous, the resulting properties will be the combination of the properties of the constituent materials. The different type of loading may call on different component of the composite to take the load. This implies that the material properties of composite materials may be different in tension and in compression as well as in bending.

In this research the focus will not be on one of the above mentioned four types only but on a hybrid class, namely laminated fiber-reinforced

composite materials as they are the basic building element of shell structures. These materials are hybrids between type 3 and type 4 since they consist of fibrous composite materials (type 3) but involve lamination techniques (type 4) in their structural composition. Typically, such materials consist of stacks of bonded-together layers made from fiber-reinforced material. The layers will often be oriented in different directions to provide specific and directed strengths and stiffnesses of the laminate. Thus, the strength and stiffnesses of the laminated fiber-reinforced composite material can be tailored to the specific design requirements of the structural element being built.

Composite materials have many mechanical behavioral characteristics which are different from those of more conventional engineering materials such as metals. More precisely, composite materials are often both inhomogeneous and non-isotropic (orthotropic or, more generally, anisotropic).

**Definitions:**

An inhomogeneous body has no uniform material properties over the body, i.e., the properties depend on position in the body. An orthotropic body has material properties that are different in three mutually perpendicular directions at a point in the body and, further, has three mutually perpendicular planes of material property symmetry. Thus, the properties depend on orientation at a point in the body.

An anisotropic body has material properties that are different in all directions at any point in the body. No planes of material property symmetry exist. Again, the properties depend on orientation at a point in the body.

These properties of composite materials significantly alter their response to loading compared to isotropic materials. Because of the inherent heterogeneous nature of composite materials, they can be studied from a micromechanical or a macromechanical point of view. When a

macromechanical point of view is taken, the material is presumed homogeneous and the effects of the constituent materials are detected only as averaged apparent macroscopic properties of the composite material. This approach is generally accepted when modeling gross response of composite structures.

## 2.2 The Composite Lamina

The basic building block of a laminated fiber-reinforced composite material is the composite lamina. A lamina is a flat or sometimes curved, as in a shell arrangement, of unidirectional or woven fibers in a supporting matrix, see Figure (2.1).

The following demands must be made on fibers used in reinforced composite materials:

1. high tensile strength
2. high modulus of elasticity
3. lower ultimate elongation than the matrix
4. good adhesion to the matrix
5. good resistance to the matrix and its additives

The influence of the matrix on the composite is as follows:

1. bind the reinforcement and distributes the load, protect the fibers chemical damage ,
2. dominant factor in determining transverse shear and through–thickness properties,
3. dominant factor in determining impact resistance and fracture toughness,
4. dominant factor in determining long time (creep) response.

The purpose of this section is to provide a basic understanding of the macro-mechanical behavior of a lamina when averaged apparent mechanical properties are considered.

## 2.3 Constitutive Relation of Lamina

The materials are assumed to behave linearly elastic, i.e. the generalized

Hooke's law is used for relating stresses to strains. A material coordinate system $1-2$ and a Cartesian coordinate system $x-y$ are introduced for the unidirectional reinforced lamina, see Figure (2.1).

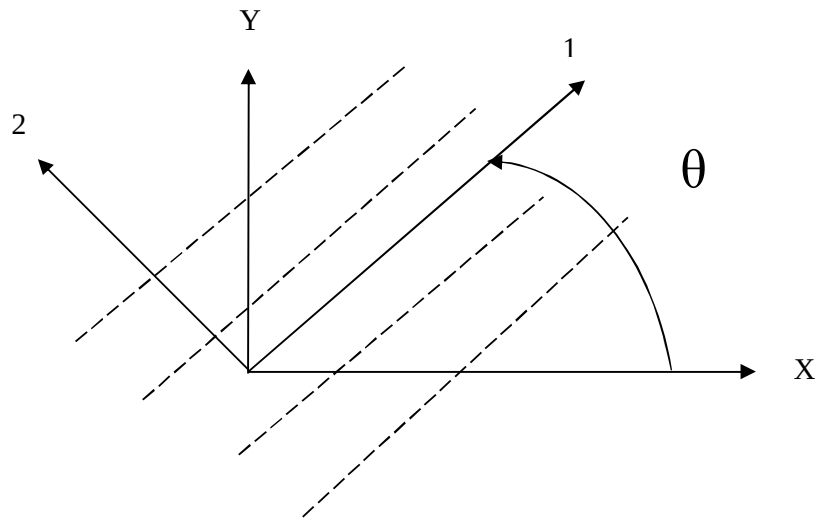


Figure (2.1) Positive notation of Principal Material Axes 1-2 from Cartesian coordinate x-y axes (Fibers are represented by dashed lines)

The general anisotropic constitutive relation is given by Hooke's law as:

$$\begin{Bmatrix} \sigma_1 \\ \sigma_2 \\ \sigma_3 \\ \tau_{23} \\ \tau_{13} \\ \tau_{12} \end{Bmatrix} = \begin{bmatrix} c_{11} & c_{12} & c_{13} & c_{14} & c_{15} & 16 \\ & c_{22} & c_{23} & c_{24} & c_{25} & c_{26} \\ & & c_{33} & c_{34} & c_{35} & c_{36} \\ & & & c_{44} & c_{45} & c_{46} \\ & \textit{symmetric} & & & c_{55} & c_{56} \\ & & & & & c_{66} \end{bmatrix} \begin{Bmatrix} \varepsilon_1 \\ \varepsilon_2 \\ \varepsilon_3 \\ \gamma_{23} \\ \gamma_{13} \\ \gamma_{12} \end{Bmatrix} \tag{2.1}$$

i.e., twenty one independent material constants are used to describe the material.

For the composite lamina illustrated in Figure (2.1), there are two orthogonal planes of material property symmetry and the material is termed orthotropic. The stress-strain relations in coordinates aligned with principal material directions are given as:

$$\begin{Bmatrix}\sigma_1\\ \sigma_2\\ \sigma_3\\ \tau_{23}\\ \tau_{13}\\ \tau_{12}\end{Bmatrix} = \begin{bmatrix} c_{11} & c_{12} & c_{13} & 0 & 0 & 0 \\ & c_{22} & c_{23} & 0 & 0 & 0 \\ & & c_{33} & 0 & 0 & 0 \\ & & & c_{44} & 0 & 0 \\ & \textit{symmetric} & & & c_{55} & 0 \\ & & & & & c_{66} \end{bmatrix} \begin{Bmatrix}\varepsilon_1\\ \varepsilon_2\\ \varepsilon_3\\ \gamma_{23}\\ \gamma_{13}\\ \gamma_{12}\end{Bmatrix} \tag{2.2}$$

If a plane stress assumption is used for the orthotropic composite lamina, the stress-strain relations will be given as:

$$\begin{Bmatrix}\sigma_1\\ \sigma_2\\ \tau_{12}\end{Bmatrix} = \begin{bmatrix} Q_{11} & Q_{12} & 0 \\ Q_{12} & Q_{22} & 0 \\ 0 & 0 & Q_{66} \end{bmatrix} \begin{Bmatrix}\varepsilon_1\\ \varepsilon_2\\ \gamma_{12}\end{Bmatrix} \tag{2.3}$$

Where:

$$\left.\begin{aligned} Q_{11} &= E_{11} / (1 - \nu_{12}\,\nu_{21}) \\ Q_{22} &= E_{22} / (1 - \nu_{12}\,\nu_{21}) \\ Q_{11} &= \nu_{12} E_{22} / (1 - \nu_{12}\,\nu_{21}) = \nu_{21} E_{11} / (1 - \nu_{12}\,\nu_{21}) \\ Q_{66} &= G_{12} \end{aligned}\right\} \tag{2.4}$$

The number of independent material constants is now reduced to four.

To express the stress-strain relations for the lamina of arbitrary orientation as illustrated in Figure (2.1),and recalling the transformation equations, the stresses in a $x-y$ coordinate system are expressed in terms of stresses in a $1-2$ coordinate system as follows:

$$\begin{Bmatrix}\sigma_x\\ \sigma_y\\ \tau_{xy}\end{Bmatrix} = T^{-1} \begin{Bmatrix}\sigma_1\\ \sigma_2\\ \tau_{12}\end{Bmatrix} \tag{2.5}$$

where;

T is transformation matrix given by:

$$T = \begin{bmatrix} a^2 & b^2 & 2ab \\ b^2 & a^2 & -2ab \\ -ab & ab & a^2 - b^2 \end{bmatrix} \tag{2.6}$$

in which

$$a = \cos\theta$$
$$b = \sin\theta$$

Θ is the orientation angle of lamina direction

In the transformation of strains it is, of course, important to realize that the above stress transformation is only valid for a second order tensor, i.e., engineering strain vectors cannot be used directly, it will be transformed to tensor strains. However, introducing the **Reuter** matrix:

$$R = \begin{bmatrix} 1 & 0 & 0 \\ 0 & 1 & 0 \\ 0 & 0 & 2 \end{bmatrix} \tag{2.7}$$

the transformation of strains can be written in compact form using both tensor and engineering notation for the strain tensor:

$$\begin{Bmatrix} \varepsilon_x \\ \varepsilon_y \\ \frac{1}{2}\gamma_{xy} \end{Bmatrix} = T^{-1} \begin{Bmatrix} \varepsilon_1 \\ \varepsilon_2 \\ \frac{1}{2}\gamma_{12} \end{Bmatrix} \tag{2.8}$$

Or

$$\begin{Bmatrix} \varepsilon_x \\ \varepsilon_y \\ \gamma_{xy} \end{Bmatrix} = R\,T^{-1}R^{-1} \begin{Bmatrix} \varepsilon_1 \\ \varepsilon_2 \\ \gamma_{12} \end{Bmatrix} \tag{2.9}$$

Using the above transformations, the stress-strain relations for arbitrary lamina orientation can be written as:

$$\begin{Bmatrix} \sigma_x \\ \sigma_y \\ \tau_{xy} \end{Bmatrix} = \begin{bmatrix} \overline{Q_{11}} & \overline{Q_{12}} & \overline{Q_{16}} \\ \overline{Q_{12}} & \overline{Q_{22}} & \overline{Q_{26}} \\ \overline{Q_{16}} & \overline{Q_{26}} & \overline{Q_{66}} \end{bmatrix} \begin{Bmatrix} \varepsilon_x \\ \varepsilon_y \\ \gamma_{xy} \end{Bmatrix} \tag{2.10}$$

where

$$\overline{Q} = T^{-1} Q R T R^{-1} \tag{2.11}$$

A specially orthotropic composite lamina is one for which the principal material axes are aligned with the structural axes. For example:

$$\begin{bmatrix} \overline{Q_{11}} & \overline{Q_{12}} & \overline{Q_{16}} \\ \overline{Q_{12}} & \overline{Q_{22}} & \overline{Q_{26}} \\ \overline{Q_{16}} & \overline{Q_{26}} & \overline{Q_{66}} \end{bmatrix} = \begin{bmatrix} Q_{11} & Q_{12} & 0 \\ Q_{12} & Q_{22} & 0 \\ 0 & 0 & Q_{66} \end{bmatrix} \tag{2.12}$$

Finally, a generally orthotropic composite lamina is an orthotropic lamina in which the principal material axes are not aligned with the structural axes. Thus the Q matrix is uniquely defined by four material properties even though the matrix is apparently that of an anisotropic material. That is:

$$Q = \begin{bmatrix} \overline{Q_{11}} & \overline{Q_{12}} & \overline{Q_{16}} \\ \overline{Q_{12}} & \overline{Q_{22}} & \overline{Q_{26}} \\ \overline{Q_{16}} & \overline{Q_{26}} & \overline{Q_{66}} \end{bmatrix} \tag{2.13}$$

These stress-strain relations for a composite lamina of arbitrary orientation are best illustrated by figures, and as examples the components of the matrix Q for a graphite epoxy are as shown in Figure (2.2) and Figure (2.3).

From Figure (2.2) and Figure (2.3) it can be clearly seen that directional dependencies of stiffness (and strength) are vital properties when designing with composite materials.

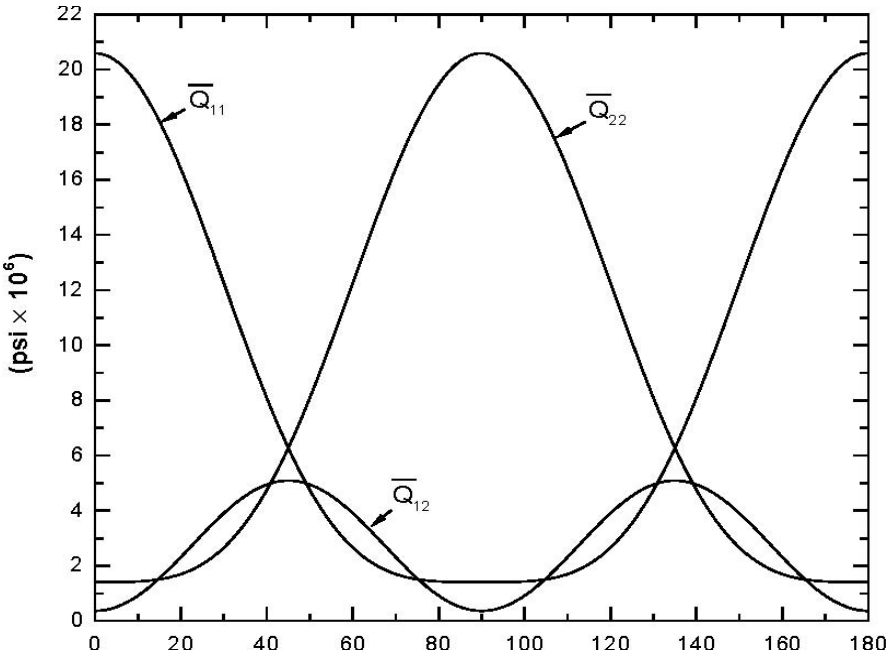


Graphite/Epoxy (3M SP-288/T300)

Figure (2.2) Results for Graphite Epoxy for Q11,Q22 and Q12

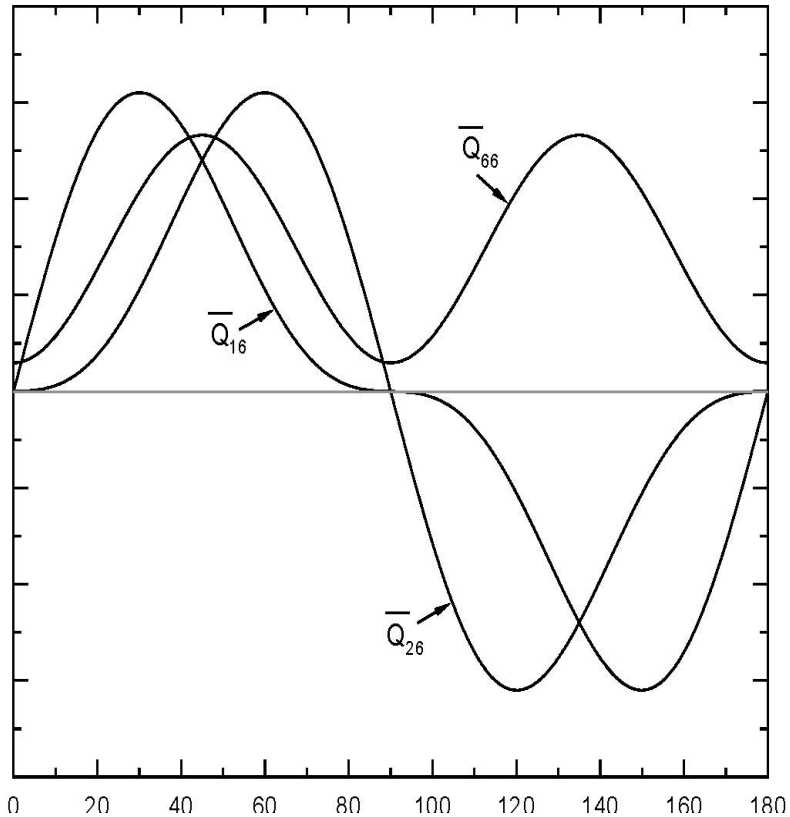

Lamina Orientation (deg)

Graphite/Epoxy (3M SP-288/T300)

Figure (2.3) Results for Graphite Epoxy for Q11,Q22 and Q12

## 2.4 Laminate Theory

A laminate is a series of laminae bonded together to act as an integral structural element. Thus, a laminate is not a material but instead a structural element with essential features of both material properties and geometry. The stiffnesses and strengths of such a composite material structural configuration are obtained from the properties of the constituent laminae, and the macromechanical behaviour of a laminate is the main topic of this section. The lamination theory described can be considered as a single layer "rule of mixtures" representation of the interaction between the multiple laminae in a plate or shell.

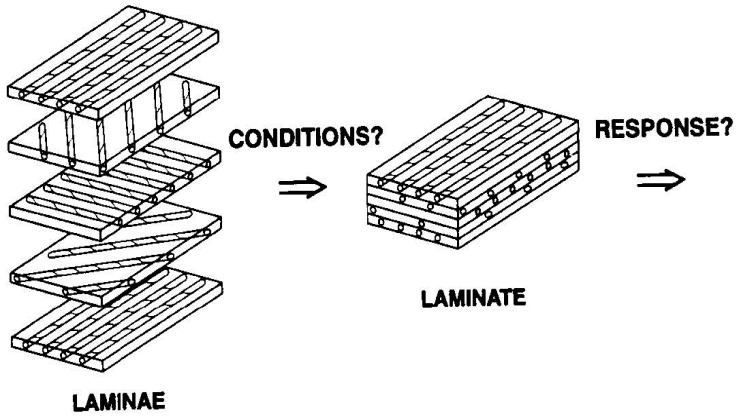


Figure (2.4) Lamina and Laminate

As illustrated in Fig. (2.4) the individual laminae may have arbitrary orientations, and the major purpose of lamination is to tailor the directional dependence of stiffness and strength of a composite material to match the loading environment of the structural element. The layers of the laminate are usually bonded together by the same matrix material that

is used in the individual laminae, i.e., in the following it is assumed that each layer is a fiber-reinforced composite lamina.

### 2.4.1 Classical Laminated Plate Theory

Classical laminated plate theory (CLPT) is often also called Classical Lamination Theory and can be regarded as a process of finding effective and reasonably accurate simplifying assumptions that reduces the three-dimensional elasticity problem to a solvable two-dimensional problem. See Figure (2.5) and Figure (2.6)

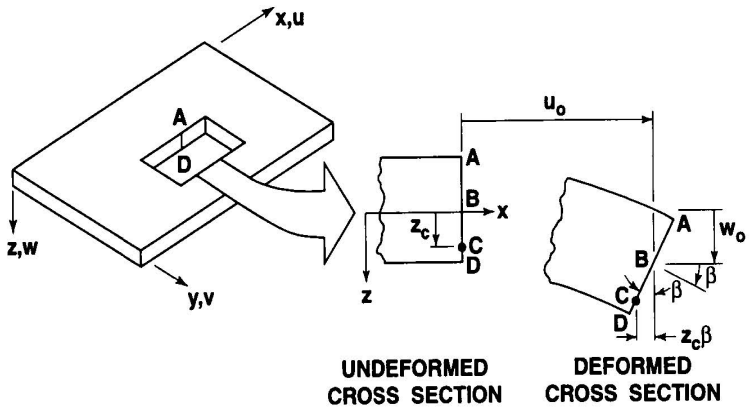


Figure (2.5) Geometry of deformation in the x-z plane

The assumptions of classical laminated plate theory are based on the Kirchhoff-Love hypothesis for plates and shells:

1. The plate is thin. The thickness ($h$) of the plate is small compared to the other physical dimensions.
2. The displacements $\bar{u}(x,y,z), \bar{v}(x,y,z)$ & $\bar{w}(x,y)$ are small compared to the plate thickness.
3. The in–plane strains $\varepsilon_x, \varepsilon_y$ & $\gamma_{xy}$ are small compared to unity

4. The transverse normal strain $\varepsilon_z$ is negligible.

5. The transverse shear stresses $\tau_{xz}$ & $\tau_{yz}$ are negligible.

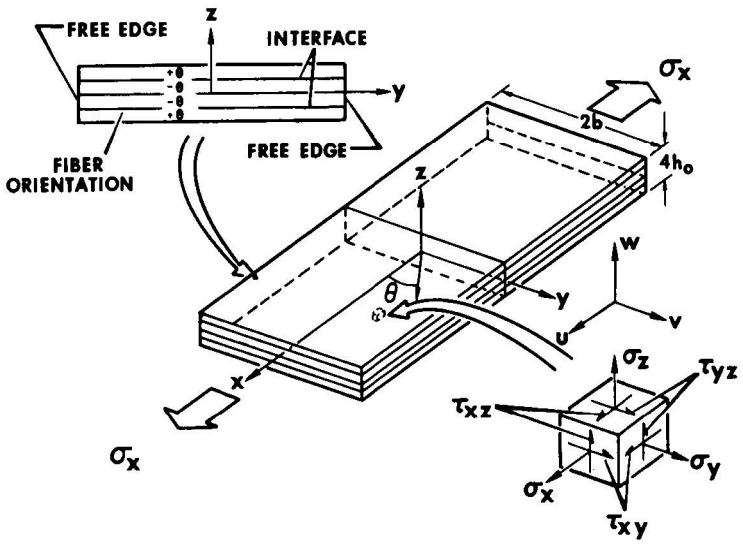


Figure (2.6) Symmetric angle-ply laminate geometry and stresses

The displacement field in case of linear elasticity is given as:

$$\left.\begin{aligned} u &= u_\circ - z\frac{\partial w}{\partial x} \\ v &= v_\circ - z\frac{\partial w}{\partial y} \\ w &= w_\circ \end{aligned}\right\} \qquad (2.14)$$

where:

$u, v$ & $w$: are displacements of point (x, y & z)

$u_\circ, v_\circ$ & $w_\circ$: are middle-surface displacements

$z$: distance normal to neutral surface

$\frac{\partial w}{\partial x}$ & $\frac{\partial w}{\partial y}$ : are normal to middle-surface rotation (slopes)

Performing force moment resultant, the constitutive relation of laminated

plate can derived as:

$$\begin{Bmatrix} N \\ M \end{Bmatrix} = \begin{bmatrix} A & B \\ B & D \end{bmatrix} \begin{Bmatrix} \varepsilon \\ k \end{Bmatrix} \tag{2.15}$$

where

$N$ & $M$ are force and moment resultants ( $N_x, N_y, N_{xy}, M_x, M_y, M_{xy}$ )

$\varepsilon$ & $k$ are middle-surface strains and curvatures( $\varepsilon_x, \varepsilon_y, \gamma_{xy}, k_x, k_y, k_{xy}$ )

$$\left.\begin{aligned} A_{ij} &= \sum_{k=1}^{N} (\overline{Q_{ij}})_k (z_k - z_{k-1}) && , i, j = 1,2,6 \\ B_{ij} &= \frac{1}{2} \sum_{k=1}^{N} (\overline{Q_{ij}})_k (z^2{}_k - z^2{}_{k-1}) && , i, j = 1,2,6 \\ D_{ij} &= \frac{1}{3} \sum_{k=1}^{N} (\overline{Q_{ij}})_k (z^3{}_k - z^3{}_{k-1}) && , i, j = 1,2,6 \end{aligned}\right\} \tag{2.16}$$

The stress evaluation in each layer k is given as:

$$\begin{Bmatrix} \sigma_x \\ \sigma_y \\ \tau_{xy} \end{Bmatrix}_k = \begin{bmatrix} \overline{Q_{11}} & \overline{Q_{12}} & \overline{Q_{16}} \\ \overline{Q_{12}} & \overline{Q_{22}} & \overline{Q_{26}} \\ \overline{Q_{16}} & \overline{Q_{26}} & \overline{Q_{66}} \end{bmatrix}_k \begin{Bmatrix} \varepsilon_x + z_k k_x \\ \varepsilon_y + z_k k_y \\ \gamma_{xy} + z_k k_{xy} \end{Bmatrix} \tag{2.17}$$

K is measured from the top of the plate as shown in Figure (2.7)

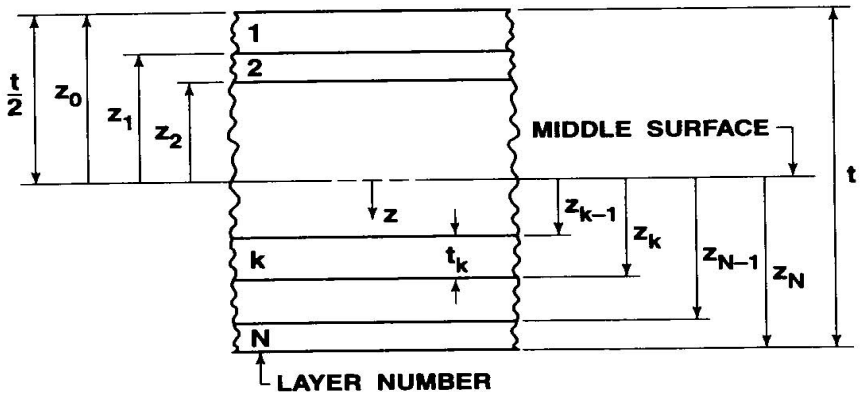


Figure (2.7) Geometry of an N-layered laminate

The advantages and disadvantages of the classical laminated theory may be summarized as follows:

• Advantages

1. Simple extension of isotropic plate theory.
2. Computer codes designed for isotropic plates can be easily modified to do composite analysis.
3. Gives excellent results for many problems. Particularly true if the results involve average structural properties.

• Disadvantages:

1. Transverse shear stresses are assumed to be zero, i.e. cannot predict delamination (separation).
2. Stress equilibrium is not satisfied across ply interfaces, which is an unrealistic result.

## 2.4.2 First order Shear Deformation Theory

The first order shear deformation theory (FSDT) is based on Reissner-Mindlin plate theory. The basic assumptions made are the same as those of classical laminated plate theory but here normal to the middle surface before deformation is no longer remain normal after deformation.

Performing force and moment resultant formulation, constitutive equation is obtained as:

$$\begin{Bmatrix} N \\ M \\ Q \end{Bmatrix} = \begin{bmatrix} A & B & 0 \\ B & D & 0 \\ 0 & 0 & \overline{A} \end{bmatrix} \begin{Bmatrix} \varepsilon \\ k \\ \gamma \end{Bmatrix} \tag{2.18}$$

Where:

$$\left.\begin{aligned} A_{ij} &= \sum_{k=1}^{N} (\overline{Q_{ij}})_k (z_k - z_{k-1}) && i, j = 1,2,6 \\ B_{ij} &= \frac{1}{2}\sum_{k=1}^{N} (\overline{Q_{ij}})_k (z^2{}_k - z^2{}_{k-1}) && i, j = 1,2,6 \\ D_{ij} &= \frac{1}{3}\sum_{k=1}^{N} (\overline{Q_{ij}})_k (z^3{}_k - z^3{}_{k-1}) && i, j = 1,2,6 \\ \overline{A}_{ij} &= \sum_{k=1}^{N} (\overline{Q_{ij}})_k (z_k - z_{k-1}) && i, j = 4,5 \end{aligned}\right\} \tag{2.19}$$

Solving above equation, the stress in each layer can be computed.

### 2.4.3Third order Shear Deformation Theory

The classical laminated plate theory and the first order shear deformation theory are the simplest equivalent single layer theories, describing adequately the kinematic behavior of most laminates. The higher order shear deformation theories avoid the use of shear correction factors. Various theories were proposed in the literature. The displacement field will be of the form

$$u = u_{\circ} + z\theta + z^3\theta^* \qquad (2.20)$$

Here, $\theta^*$ represents the higher order rotations.

An improved higher order shear deformation theory equivalent to single layer theory which better accounts for transverse effects is that has been proposed by Reddy [4] for laminated shells, but it increases computational cost dramatically at a little gain in model accuracy. To significantly improve results compared to those obtained with ESL – method, it is necessary to turn to layerwise theories.

## 2.4.4 Layerwise Theories

Layerwise theories can be divided into two categories , namely full layerwise and partial layerwise theories. The difference lies in the displacement expansions. The partial layerwise theories assume that normal transverse strain is zero where as full layerwise theories use a full expansion for all three displacements. Layerwise theories are as ESL-methods often formulated in force moment resultants.

The layerwise theory developed by Reddy [11] allows for a better deformation analysis in the laminate. In this theory the displacement field for each layer (n) is a function of the displacements of other layers adjacent, as

$$v^{(n)} = v^{(n-1)} + z\theta_y{}^{(n)}$$

$$u^{(n)} = u^{(n-1)} + z\theta_x{}^{(n)} \qquad (2.21)$$

$$w^{(n)} = w_\circ$$

The theory is implemented using degenerated shell element.

## 2.5 Finite Element Method

The solution of the governing equations of laminated composite plates and shells can be solved by analytical methods. However, exact analytical or variation solutions to this problem cannot be developed when complex geometries, arbitrary boundary conditions, or nonlinearities are involved. Therefore, approximate methods of analysis become relevant when there is a need for solving such problems.

The finite element method is a powerful numerical technique for the solution of differential and integral equations that rise in various fields of engineering and applied science. The basic idea of the finite element method is to view a given domain as an assembled set of simple geometries, called finite elements, for which it is possible to generate element properties (stiffness matrix and nodal load vectors) using any energy or variation method. The major steps of the finite element method include: the discretization of the domain into a set of finite elements (mesh); computation of element stiffness matrix and nodal load vectors using energy method; assembly of elements to obtain a global system of algebraic equations; imposition of boundary conditions; solutions of equations and calculation of element stresses.

## 2.6 Finite Elements for Analysis of Laminated Shell Structures:

Here some laminated shell finite elements formulations developed in literature are described in brief:

1. J. Stegmann et al [23], developed a degenerated nonlinear stabilized formulation, it gives satisfactory results but the computation is very expensive due to the through thickness integration scheme adopted.
2. Prema Kumar [21], in his PhD thesis proposed an efficient integration scheme by assuming a variation of Jacobian matrix through thickness but his formulation is unstable because no account for shear locking is made.
3. Klinkel et al. [40] formulate a solid element with MITC and Enhanced Assumed Strain (EAS) stabilization for non-linear analysis of ESL composite laminates.
4. Masud and Panahandeh [41] proposed an element similar to the above element in [3] for linear analysis of composite laminates but utilized reduced and selective integration.
5. Brank and Carrera [1] suggested a layerwise degenerated element with Assumed Natural Strain (ANS) stabilization for linear analysis.
6. Alfano et al.) [30] Formulated a MITC element with out-of-plane stress capabilities for linear analysis of ESL plates.
7. H. Nguyen [14] developed a new simple accurate four node quadrilateral element for linear static and dynamic analysis of thin to moderately thick laminated anisotropic plate/shell structures within the first-order shear deformation theory.
8. M.L. Liu [27 ] developed a geometrically nonlinear analysis of layerwise anisotropic shell structures by hybrid strain based lower order elements. The shell element employed has three nodes located at mid-surface of the shell and eighteen degrees-of-freedom. The nodal degrees-of-freedom at each node are three translational and three rotational degrees-of-freedom

9. N. Al-Ghamdy [29 ] developed a geometrically nonlinear finite element formulation of a four node isoparametric laminated shell element based on a cube displacement field over the shell thickness .
10. P. Mohan [31] combined plane bending element with memberane element to analyze laminated plate and shell structures. The utilized element possesses six degrees of freedom**.**
11. H. S. Kim [6] formulated an efficient layerwise shear deformation theory for improving the accuracy of stress and strain prediction in the analysis of laminated shells.
12. B. Wang [39] developed flat triangular shell elements for geometrically nonlinear static and dynamic analysis of large scale laminated composite plate and shell structures. Each element, based on the first – order shear deformation theory, has three nodes and each node has six degrees of freedom. The updated Lagrangian formulation and modified incremental Hellinger-Reissner variational principle were adopted.

Other contributions have proposed elements with similar characteristics, some of which are listed in Reddy [11]. Creating a complete overview of advance element formulations for laminated structures is difficult since new elements arrive continuously. The general trend tends towards stabilized elements and still more towards layerwise theories or at least some form of assumed transverse displacement field.

## 2.7 Locking Problems

When displacement based elements are formulated the decisive and crucial choice is the choice of interpolation functions (as described earlier). If the interpolation chosen cannot model the behavior of the real structure sufficiently accurate, the response of the model may not only be inaccurate but incorrect. Locking occurs when the finite element model

becomes overly stiff in comparison with the real structure. Locking may occur in various loading situations and several locking problems may arise simultaneously or single phenomenon may appear isolated. This renders the identification of locking very difficult for an engineer reviewing the results of a finite element analysis. Therefore, the need arises for stable, locking free elements.

The problems and solutions of locking are treated in general terms by Bathe [1]. In the following a brief introduction will be given to three locking phenomena and possible solution strategies will be presented.

### 2.7.1 Membrane Locking

Membrane locking is only a problem in curved beam and shell elements, If considering a shell, the membrane stiffness is very large compared to the bending stiffness and the shell may therefore bend without stretching. This is called inextensional bending and membrane locking is caused by the elements inability to represent this type of bending. This means that when the element is loaded in pure bending parasitic membrane stresses may be introduced whereby the element exerts overly stiff behavior. Since membrane locking only occurs in curved elements (such as 6,-8-or 9-node elements) it is not necessary to address the problem when formulating 3-and 4-node elements since these elements are plane. To make curved elements reliable it is therefore necessary to consider membrane locking when formulating such elements.

The solution to membrane locking is to modify the interpolation of the in-plane stresses. These modifications can be made in various ways such as the Enhanced Assumed Strain-method (EAS) or by (MITC) [6].

### 2.7.2 Shear Locking

Shear locking is a problem for many types of elements. Shear locking is a result of parasitic transverse shear stresses introduced when the element is loaded in bending. In a state of pure bending, resulting from application of a constant moment, M, the shear force is the derivative of the moment,

i.e. V= ∂M/∂xi. Hence, for constant moment the shear force is zero. Using a Timoshenko beam analogy (which is reasonable since the Mindlin assumptions for shells constitute the same restrictions as made by Timoshenko for beams) the shear stress is given from the shear formula, stated here as $\sigma 13 = V\gamma$, where γ is a geometric quantity. Consequently, the shearing stresses must be zero since the shear force is zero for constant bending moment. Shear locking occurs when the element is unable to calculate zero transverse shearing stresses in pure bending. It may also arise when applying a linearly varying moment to an element if the element in this case is unable to determine constant transverse shearing stresses. The former is a problem in first-order elements and the latter in second-order elements; this is explained in the following section.

For the linear elements shear locking arises since the elements are incapable of representing the deformation caused by pure bending. This is shown in Figure (2.8) where an edge view of a deformed linear element is shown in Figure( 2.8a) and a correct deformed geometry is shown in Figure (2.8b)

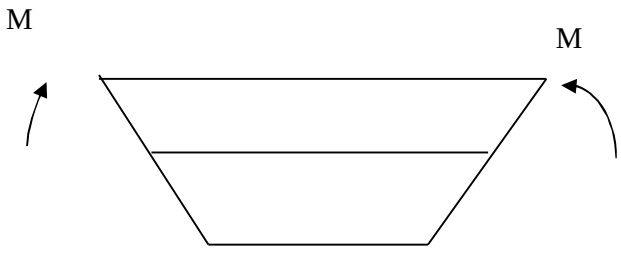


Figure (2.8a)

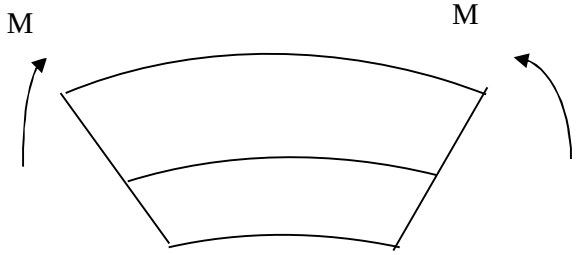


Figure (2.8b)

Figure (2.8) Edge view of (a) deformed linear element, (b) correct deformed geometry in pure bending

If quadratic elements are considered instead, because of the mid-side node, properly represent the deformation caused by pure bending. In the quadratic elements the parasitic transverse shear stress instead arises

when the elements are loaded under linearly varying bending. Since shear locking is a problem in many elements a lot of different methods have been developed to eliminate it. For all the improvement methods shear locking is avoided by modifying the determination of the transverse shear stresses. This means that the last two rows in the strain-displacement matrix, B, are modified.

### 2.7.3 Volumetric and Thickness Locking

Volumetric locking is different from other locking problems in that volumetric locking is caused by a material parameter namely the Poisson ratio, ν, volumetric locking appears for isotropic materials when the material becomes incompressible or nearly incompressible, i.e. meaning ν tends to 0.5. This may be realized from Hooke's generalized law rewritten from Equation (2.1) for isotropic materials:

$$\sigma_{ij} = \lambda \delta_{ij} \varepsilon_{kk} + 2\eta \varepsilon_{ij} \tag{2.22}$$

Where; $\lambda$ and $\eta$ are Lame's constants given as

$$\lambda = \frac{E}{(1+\nu)(1-2\nu)} \qquad \eta = \frac{E}{2(1+\nu)} \tag{2.23}$$

Considering, $\lambda$, it is seen that when ν tends to 0.5 then λ tends to infinity . This means that some of the terms in the constitutive matrix tend towards infinity and in turn, terms in the stiffness matrix tend towards infinity.

Considering the modified constitutive matrix in Eqn.(2.6) it can be seen that none of the terms reaches infinity when $\nu \rightarrow 0.5$. The reason is that the modified constitutive matrix has been derived for reduced state of

stress for which the term $(1-2\nu)$ vanishes.

For orthotropic materials it may be seen from Eqn. (2.6) that terms in the constitutive matrix may reach infinite if $\nu \to 1$. If considering a single layer (stacks of layers may have entirely different material properties when viewed as a whole) it seems reasonable to conclude that for common engineering materials and the case of linearly elastic materials this will never be the case. For this reason volumetric locking does not represent a problem in the formulated elements and hence, this locking phenomenon is not treated any further.

Besides the three locking phenomena explained in the preceding sections two different thickness locking phenomena exist, namely thickness locking and curvature thickness locking. Both of these locking effects are caused by a parasitic transverse normal stress and therefore only appear when thickness changes are taken into account in the shell formulation. This means that for the five parameter formulation (the Mindlin assumption) used in the implemented shell elements these two types of locking will not come into effect. Consequently, no strives towards eliminating such locking problems are taken in the formulation of the shell elements.

## 2.8 Geometrically Nonlinear Formulation

All geometrically nonlinear formulations stated earlier are based on Green strains, since, most of the material constants and constitutive relations are based on Engineering stress, geometric strains, which are work-conjugate will be suitable to use, specially for large rotation problem Mohamed A. E [19], Adam F. M. [18] used Green strain formulations in the analysis of beams, shells and plane stress/strain structures respectively.

Most recent researches use Green's strain in formulating problems, in this research Geometric strain will be used beside Green's strain , and in

further studies other strain measure will be used e.g. Logarithmic strain

## 2.10 Conclusion

In view of the above mentioned theories and formulations, it was observed that most of them are adopting Green's strains. In this study an eight node degenerated shell finite element is formulated adopting total Lagrangian formulation and using both Green strains and geometric strains. The element formulated is implemented to analyze laminated shell structures using full numerical integration through thickness. The nonlinear equations are solved using Newton – Raphson method.

# CHAPTER THREE

# LINEAR FINITE ELEMENT ANALYSIS OF LAMINATEDE SHELLS

## 3.1 Introduction

Generally shell structures could be considered as those structures having small thickness compared with their other dimensions. Shells may be flat such as plates or curved like cylindrical shells and domes. They can be made from concrete, steel or any other material. The advantage of shell is that it can cover a large area with long spans such as large halls or stadia .Shell structures get their strength by their shape not by the high strength of their constructing materials.

Curved shell structures such as domes are considered as economic structures because they are capable in translating applied loads into membrane thrusts and shears acting in a plane tangential to the surface at any point. By this means bending and twisting moments and shears transverse to the surface are reduced or eliminated.

### 3.2 Finite Element Method

Finite Element Method of analysis (FEM) is a computer–based numerical technique for calculating the strength and behavior of engineering structures. The finite element method has been widely used in many branches of science and engineering. The most common applications are found in solid mechanics. It has the advantage of solving problems with different materials and boundaries, with the advantage of computer programming and modeling, problems may be static or dynamic. The

most widely used finite element formulation in solid mechanics is the displacement approach. The displacement field within the element is defined in terms of assumed functions (interpolation functions) and unknown parameters at the nodes which are either displacements or displacement related quantities such as slopes and curvatures.

In finite element method, a structure is broken down into small simple **blocks** or **elements**. The behavior of an individual element can be described with a relatively simple set of equations. Just as the set of elements would be joined together to build the whole structure, the equations describing the behaviors of the individual elements are joined into an extremely large set of equations that describe the behavior of the whole structure. The computer can solve this large set of simultaneous equations. From the solution, the computer extracts the behavior of the individual elements. From this, it can get the stress and deflection of all parts of the structure.

The steps of a displacement-based finite element analysis [8] can be summarized as follows:

1. Discretization (or representation) of the given domain into a collection of preselected finite elements.
2. Selection of nodal displacement parameters and element interpolation function.
3. Evaluation of individual element properties.
4. Assembly of system overall stiffness matrix.
5. Imposition of boundary condition.
6. Formation of global right hand side (r. h. s) force vector.
7. Solution of system matrix equations for nodal displacements.
8. Additional calculation for stresses and other parameters.

### 3.3 Historical Background

The finite element concept was introduced in the classical paper presented by Turner, Cough, Martin and Top in 1956. After this paper and other researches an explosive development of finite element method started. It appears that Clough was the first to use the terminology finite element in 1960. Due to rapid development in computer technology large number of

package programs have been developed for finite element analysis e.g. Structural Analysis Program (**SAP2000**).

The method began as numerical techniques for analyzing solid mechanics continuum and then extended to solve heat conduction, fluid flow and magnetic field problems in both states, static and dynamic.

### 3.4 Types of Analyses of Structures

Types of analyses of structures can be classified into four categories:

1- Small deflection and elastic material properties (linear analysis).
2- Small deflection and plastic material properties (material non-linearity).
3- Large deflection (deformation) and elastic material properties (geometric non-linearity).
4- Simultaneous large deflection and plastic material properties (combination of material and geometric non-linearity).

Material nonlinearity means that stress strain relationship is non- linear. Geometric nonlinearity (large deflection), means that the shape of the structure has changed enough that the relationship between applied load and deflection is no longer a simple straight line relationship. The material properties can still be elastic.

In addition to analyzing structures for their stress and deflection, other typical analyses are an evaluation of the natural frequency of vibration, and calculation of buckling loads. Steady state, transient, and random vibration behavior can also be analyzed.

For this research we shall study the case of geometric non-linearity. Loads may be due to self weight, normal pressure, concentrated loads, surface pressure or initial stress or strain.

### 3.5 Degeneration Method

The degeneration method is a very "inexpensive" way of formulating shell finite elements and has been the leading method ever since it was introduced in 1970 by Ahmad et al. (1970) [38]. Basically, the method starts from a standard 3D continuum solid element (hence continuum based shell elements) and, by enforcing various constraints on the element behavior, arrives at a 2D shell element. The procedure of the method is to eliminate nodes in the 3D continuum element by enforcing different constraints on the behavior of the element. An 8-node degenerated element can for example be constructed from a solid 20 node brick. Assumptions introduced in the formulation are:

1- Lines normal to the mid-surface before deformation remain normal after deformation
2- Transverse normal stress is zero

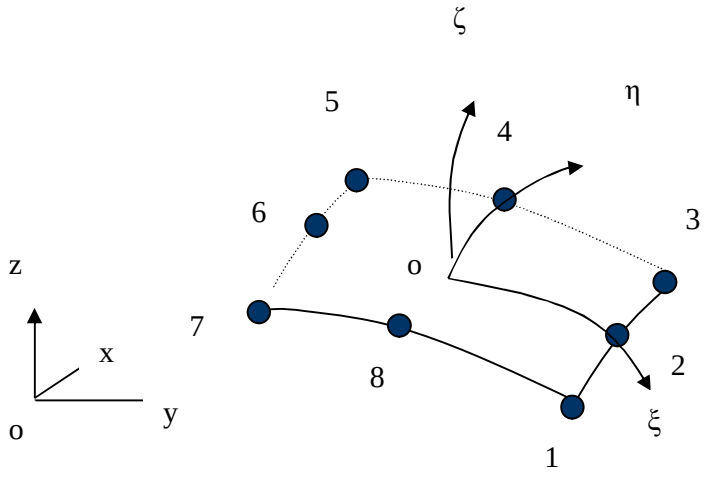


Figure (3.1) Eight node curved element

### 3.5.1 Geometry of the Element

Figure (3.1) shows an eight node Serenpdity element. Adopting isoparametric concept, the shape functions defining the geometry and variation of displacement are given by:

For nodes 1, 3,5and7

$$N_i = 0.25\,(1+\xi\xi_i)(1+\eta\eta_i)(\xi\xi_i+\eta\eta_i-1) \qquad (3.1)\ a$$

For nodes 2, 6

$$N_i = 0.5\,(1+\xi^2)(1+\eta\eta_i) \qquad (3.1)\ b$$

For nodes 4, 8

$$N_i = 0.5\,(1+\eta^2)(1+\xi\xi_i) \qquad (3.1)\ c$$

where:

$\xi$ , $\eta$ *and* $\zeta$ : are natural coordinates

$\xi_i$ , $\eta_i$ *and* $\zeta_i$: are the values of natural coordinates at node $i$ .

$N_i$: shape function at node $i$ .

Assuming the lines joining the top and bottom nodes to be straight, the shape of the element is defined by eight nodal values as:

$$\begin{Bmatrix} x \\ y \\ z \end{Bmatrix} = \sum_{i=1}^{8} N_i \left[ \begin{Bmatrix} x_i \\ y_i \\ z_i \end{Bmatrix} + \zeta_i \frac{t_i}{2} v_{3i} \right] \qquad (3.2)\ a$$

where,

$x$ , $y$ *and* $z$ : are global axes

$x_i$ , $y_i$ *and* $z_i$ : are the global coordinates of node $i$

$t_i$ : is the shell thickness at node i

$N_i$ : shape function at node $i$ .

$v_{3i}$ : is a unit vector in the direction normal to the mid-surface plane as shown in Figure (3.2) and defined by:

$$v_{3i} = \begin{Bmatrix} x_i \\ y_i \\ z_i \end{Bmatrix}_{top} - \begin{Bmatrix} x_i \\ y_i \\ z_i \end{Bmatrix}_{bottom} = \begin{Bmatrix} x^*_i \\ y^*_i \\ z^*_i \end{Bmatrix} \qquad (3.2)\ b$$

The subscripts top and bottom refer to top and bottom coordinates.

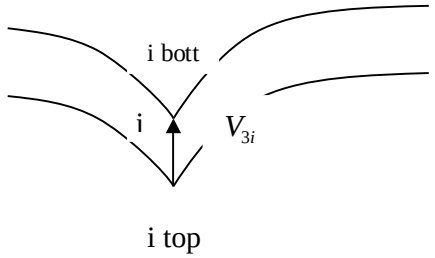


Figure (3.2) Node director

### 3.5.2 Displacement Field

According to the assumption that strains in the direction normal to the mid-surface will be assumed to be negligible, the displacement through the element will be taken to be uniquely defined by the three Cartesian components of mid-surface node displacement and two rotations of the nodal vector $V_{3i}$ about orthogonal directions that are given by vectors $V_{2i}$ and $V_{1i}$ of unit magnitude, with corresponding (scalar) rotations α and β. Thus the displacement at any point within the element can be written as:

$$\begin{Bmatrix} u \\ v \\ w \end{Bmatrix} = \sum_{i=1}^{8} N_i \left[ \begin{Bmatrix} u_i \\ v_i \\ w_i \end{Bmatrix} + \zeta_i \frac{t}{2} \begin{bmatrix} v_{1i} & v_{2i} \end{bmatrix} \begin{Bmatrix} \alpha_i \\ \beta_i \end{Bmatrix} \right] \qquad (3.3)\ a$$

where

$u$, $v$ and $w$ are global displacements at any point within element

$u_i$ , $v_i$ and $w_i$ are nodal displacements of node $i$ .

$V_{3i}$ is the vector in the direction that is normal to mid-surface, and is given by Equation (3.3).

$V_{1i}$ is perpendicular to plane defined by $V_{3i}$ and the x-axis, and is thus given by the cross-product:

$$V_{1i} = i \times V_{3i} = \begin{Bmatrix} 0 \\ -z_i^* \\ y_i^* \end{Bmatrix} \qquad (3.3)\ \text{b}$$

This process fails if $V_{3i}$ corresponds in direction with the x-axis. In this case the local directions are obtained using the y-axis.

$V_{2i}$ is normal to the $V_{1i}$ and $V_{3i}$, then

$$V_{2i} = V_{1i} \times V_{3i} = \begin{Bmatrix} -z_i^{*2} - y_i^{*2} \\ x_i^* . y_i^* \\ x_i^* . z_i^* \end{Bmatrix} \qquad (3.4)$$

By dividing vectors $V_{1i}$, $V_{2i}$ and $V_{3i}$ by their lengths, the unit vectors $v_{1i}$, $v_{2i}$ and $v_{3i}$ can be obtained respectively.

### 3.5.3 Strain - displacement Relations

The strain-displacement relations for linear analysis are given by the following equation:

$$\begin{Bmatrix} \varepsilon_x \\ \varepsilon_y \\ \gamma_{xy} \\ \gamma_{xz} \\ \gamma_{yz} \end{Bmatrix} = \begin{Bmatrix} \dfrac{\partial u}{\partial x} \\ \dfrac{\partial v}{\partial y} \\ \dfrac{\partial u}{\partial y} + \dfrac{\partial v}{\partial x} \\ \dfrac{\partial w}{\partial x} + \dfrac{\partial u}{\partial z} \\ \dfrac{\partial w}{\partial y} + \dfrac{\partial v}{\partial z} \end{Bmatrix} = [B]\{a\} \qquad (3.5)$$

Where

$[B]$: is the matrix relating strain with nodal displacements $\{a\}$: are the nodal displacements

### 3.5.4 Constitutive Relations

The stress- strain relations for three dimensional analyses is written as follows:

$$\{\sigma\} = [C]\{\varepsilon\} \qquad (3.6)$$

Where:

$\{\sigma\}^T = \begin{bmatrix} \sigma_x & \sigma_y & \tau_{xy} & \tau_{xz} & \tau_{yz} \end{bmatrix}$ Stress component

$\{\varepsilon\}^T = \begin{bmatrix} \varepsilon_x & \varepsilon_y & \gamma_{xy} & \gamma_{xz} & \gamma_{yz} \end{bmatrix}$ Strain component

$[C]$ = Elasticity matrix

For isotropic material $[C]$ is given in a matrix form as:

$$[C] = \frac{E}{(1-\upsilon^2)} \begin{bmatrix} 1 & \upsilon & 0 & 0 & 0 \\ & 1 & 0 & 0 & 0 \\ & & \dfrac{1-\upsilon}{2} & 0 & 0 \\ & \textit{symmetric} & & \dfrac{1-\upsilon}{2k} & 0 \\ & & & & \dfrac{1-\upsilon}{2k} \end{bmatrix} \qquad (3.7)$$

where

$E$ Young's modulus

$\upsilon$ Poisson's ratio

$k$ Shear correction factor, equal to 5/6 for rectangular sections

### 3.5.5 Stiffness Matrix

The element stiffness matrix is evaluated as follows

$$[K] = \int_v [B]^T [C][B]\, dv \qquad (3.8)$$

where:

$[K]$ = element stiffness matrix

$[B]$ = matrix relating strains to displacements

$[C]$ = modulus of elasticity

The integration over the volume is carried out numerically considering eight Gauss points.

### 3.5.6 Transformation Matrix

Since the expressions for stresses are obtained in the global directions, the axes $x, y, z$ system must be rotated to a set $x', y', z'$ as shown in Figure (2.2). This set of mutually perpendicular axes at the point being considered is determined from the local axes $\xi$ , $\zeta$ and $\eta$ (natural coordinate) as follows

$x'$ is identical $\xi$

$z'$ is perpendicular to $\zeta$ and $\eta$

$y'$ is perpendicular to $x'$ and $z'$

Let $v_r$ and $v_s$ be unit vector along $r$ and $s$ directions respectively, and are defined as follows

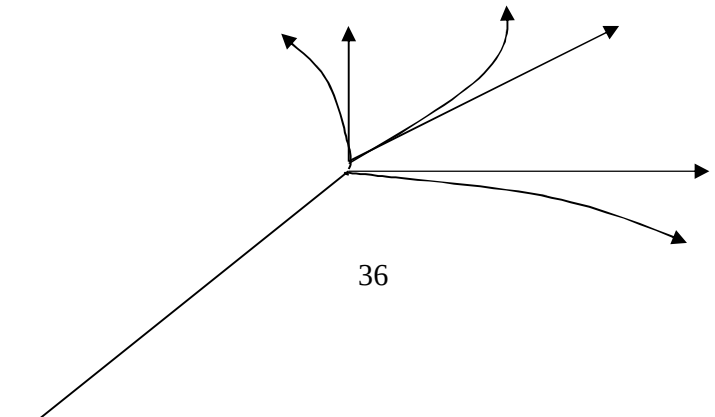

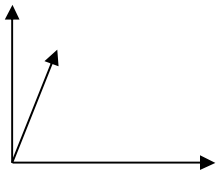

Fig. 3.3 Transformation from global to local axis

$$V_r = \begin{Bmatrix} \frac{\partial x}{\partial \xi} \\ \frac{\partial y}{\partial \xi} \\ \frac{\partial z}{\partial \xi} \end{Bmatrix} \quad ; \quad V_s = \begin{Bmatrix} \frac{\partial x}{\partial \zeta} \\ \frac{\partial y}{\partial \zeta} \\ \frac{\partial z}{\partial \zeta} \end{Bmatrix} \tag{3.9}$$

Element of vectors in Equation (3.9) are found in Jacobian matrix.

By reducing these to unit magnitudes, we define $v_r$ , $v_s$ .

Let $v_1, v_2 \,\&\, v_3$ be unit vectors along $x', y' \,\&\, z'$ respectively, and from definition of $x', y', z'$ system , we have

$V_1 = V_r$

$V_3 \perp V_r \,\&\, V_S$

$V_2 \perp V_1 \,\& V_3$

Then and from (3.9)

$$V_1 = \begin{Bmatrix} \frac{\partial x}{\partial \xi} \\ \frac{\partial y}{\partial \xi} \\ \frac{\partial z}{\partial \xi} \end{Bmatrix} \quad ; \quad V_3 = V_r \times V_s = \begin{Bmatrix} \frac{\partial y}{\partial r}\frac{\partial z}{\partial s} - \frac{\partial z}{\partial r}\frac{\partial y}{\partial s} \\ \frac{\partial x}{\partial s}\frac{\partial z}{\partial r} - \frac{\partial x}{\partial r}\frac{\partial z}{\partial s} \\ \frac{\partial x}{\partial r}\frac{\partial y}{\partial s} - \frac{\partial x}{\partial s}\frac{\partial y}{\partial r} \end{Bmatrix} \tag{3.10}$$

$$V_2 = V_3 \times V_1 = \begin{Bmatrix} \frac{\partial x}{\partial s}(\frac{\partial z}{\partial r})^2 - \frac{\partial x}{\partial r}\frac{\partial z}{\partial s}\frac{\partial z}{\partial r} - \frac{\partial x}{\partial r}\frac{\partial y}{\partial s}\frac{\partial y}{\partial r} + \frac{\partial x}{\partial s}(\frac{\partial y}{\partial r})^2 \\ \frac{\partial y}{\partial s}(\frac{\partial x}{\partial r})^2 - \frac{\partial x}{\partial s}\frac{\partial x}{\partial r}\frac{\partial y}{\partial r} - \frac{\partial y}{\partial r}\frac{\partial z}{\partial r}\frac{\partial z}{\partial s} + \frac{\partial y}{\partial s}(\frac{\partial z}{\partial r})^2 \\ \frac{\partial z}{\partial s}(\frac{\partial y}{\partial r})^2 - \frac{\partial y}{\partial s}\frac{\partial y}{\partial r}\frac{\partial z}{\partial r} - \frac{\partial x}{\partial r}\frac{\partial x}{\partial s}\frac{\partial z}{\partial r} + \frac{\partial z}{\partial s}(\frac{\partial x}{\partial r})^2 \end{Bmatrix}$$

(3.11)

By reducing vectors $V_1$ , $V_2$ & $V_3$ to unit vectors, we construct a matrix of unit vectors $v_1$ , $v_2$ & $v_3$ in the local direction, therefore

$$[T\ ] = [v_1\ ,\ v_2\ ,\ v_3]$$

Where

$T$ is the transformation matrix

In order to find the displacement derivatives w.r.t the global Cartesian co-ordinates, and making use of the relation between the global displacements $u$ , $v$ & $w$ to the curvilinear co-ordinates, the derivatives are given by a matrix relation

$$\begin{bmatrix} \frac{\partial u}{\partial x} & \frac{\partial v}{\partial x} & \frac{\partial w}{\partial x} \\ \frac{\partial u}{\partial y} & \frac{\partial v}{\partial y} & \frac{\partial w}{\partial y} \\ \frac{\partial u}{\partial z} & \frac{\partial v}{\partial z} & \frac{\partial w}{\partial z} \end{bmatrix} = [J]^{-1} \begin{bmatrix} \frac{\partial u}{\partial \xi} & \frac{\partial u}{\partial \xi} & \frac{\partial u}{\partial \xi} \\ \frac{\partial u}{\partial \zeta} & \frac{\partial u}{\partial \zeta} & \frac{\partial u}{\partial \zeta} \\ \frac{\partial u}{\partial \eta} & \frac{\partial u}{\partial \eta} & \frac{\partial u}{\partial \eta} \end{bmatrix} \qquad (3.12)$$

Where

$J$ : is Jacobean matrix defined by:

$$[J] = \begin{bmatrix} \frac{\partial x}{\partial \xi} & \frac{\partial y}{\partial \xi} & \frac{\partial z}{\partial \xi} \\ \frac{\partial x}{\partial \zeta} & \frac{\partial y}{\partial \zeta} & \frac{\partial z}{\partial \zeta} \\ \frac{\partial x}{\partial \eta} & \frac{\partial y}{\partial \eta} & \frac{\partial z}{\partial \eta} \end{bmatrix} \qquad (3.13)$$

The global derivatives of displacements $u$, $v$ & $w$ are now transformed to the local derivatives of the local orthogonal displacements by the standard operation

$$\begin{bmatrix} \frac{\partial u'}{\partial x'} & \frac{\partial v'}{\partial x'} & \frac{\partial w'}{\partial x'} \\ \frac{\partial u'}{\partial y'} & \frac{\partial v'}{\partial y'} & \frac{\partial w'}{\partial y'} \\ \frac{\partial u'}{\partial z'} & \frac{\partial v'}{\partial z'} & \frac{\partial w'}{\partial z'} \end{bmatrix} = [T]^{\mathrm{T}} \begin{bmatrix} \frac{\partial u}{\partial x} & \frac{\partial v}{\partial x} & \frac{\partial w}{\partial x} \\ \frac{\partial u}{\partial y} & \frac{\partial v}{\partial y} & \frac{\partial w}{\partial y} \\ \frac{\partial u}{\partial z} & \frac{\partial v}{\partial z} & \frac{\partial w}{\partial z} \end{bmatrix} [T] \qquad (3.14)$$

### 3.5.7 Element Load Vector

The following load types are considered

1. Gravity load.
2. Uniform surface load.
3. Uniform normal surface pressure

#### 3.5.7.1 Gravity load

The load vector due to body force at node (i) is given by:

$$\{Q_i\} = \int_v [N_i]^T \{X\} d\upsilon = \int_{-1}^{1}\int_{-1}^{1}\int_{-1}^{1} [N_i]\{X_i\} \det[J] d\xi \, d\eta \, d\zeta \qquad (3.15)$$

Where:

$\{X\}$: is the vector of body force components per unit volume. Let $\rho$ be the weight density of the material. The nodal load vector at any node $i$ is given by

$$\{X\} = \begin{Bmatrix} bx \\ by \\ bz \end{Bmatrix} = \begin{Bmatrix} 0 \\ 0 \\ -\rho z \end{Bmatrix} \qquad (3.16)$$

and

$$[N_i]=\begin{bmatrix} N_i & 0 & 0 & \frac{1}{2}N_i\zeta\, h v_{11i} & -\frac{1}{2}N_i\zeta\, h v_{21i} \\ 0 & N_i & 0 & \frac{1}{2}N_i\zeta\, h v_{12i} & -\frac{1}{2}N_i\zeta\, h v_{22i} \\ 0 & 0 & N_i & \frac{1}{2}N_i\zeta\, h v_{13i} & -\frac{1}{2}N_i\zeta\, h v_{23i} \end{bmatrix} \quad (3.17)$$

h is the thickness of the shell at point considered

$[J]$ jacobian matrix function of ( $\xi$ , $\zeta$ and $\eta$)

$\det[J]$: is determinant of Jacobean matrix

$v_{11i}$ , $v_{12i}$ and $v_{13i}$ : are components of unit vectors $v_{1i}$

$v_{21i}$ , $v_{22i}$ and $v_{23i}$ : are components of unit vectors $v_{2i}$

Hence:

$$\{Q_i\}=\int_{-1}^{1}\int_{-1}^{1}\int_{-1}^{1}\begin{Bmatrix} 0 \\ 0 \\ N_i bz \\ \zeta\, N_i \frac{h}{2} v_{13i}.bz \\ \zeta\, N_i \frac{h}{2} v_{23i}.bz \end{Bmatrix}\det[J]\, d\xi\, d\eta\, d\zeta \quad (3.18)$$

### 3.5.7.2 Uniform Surface Load

Following the same process, the element surface force due to uniform surface load is given by:

$$\{Q_i\}=\int_{-1}^{1}\int_{-1}^{1}\begin{Bmatrix} 0 \\ 0 \\ N_i Pz \\ \zeta\, N_i \frac{h_i}{2} v_{13i} Pz \\ \zeta\, N_i \frac{h_i}{2} v_{23i} Pz \end{Bmatrix}|a|\, d\xi\, d\eta \quad (3.19)$$

where ;

$P$ = uniform surface load

$|a|$ = surface Jacobean

$|a| = \|V_r x V_s\|$

at top $\zeta$ =1 and at bottom $\zeta$ = -1

### 3.5.7.3 Pressure Normal to Surface

Similarly the nodal force due to normal surface pressure is given by:

$$\{Pni\} = \int_{-1}^{1}\int_{-1}^{1} P \begin{Bmatrix} N_i v_{31} \\ N_i v_{32} \\ N_i v_{33} \\ \zeta\, N_i \dfrac{h_i}{2}(v_{11}v_{31} + v_{12}v_{32} + v_{13}v_{33}) \\ -\zeta\, N_i \dfrac{h_i}{2}(v_{21}v_{31} + v_{22}v_{32} + v_{12}v_{33}) \end{Bmatrix} |a|\, d\xi\, d\eta \qquad (3.20)$$

$P$ = normal surface load.
at top $\zeta$ =1 and at bottom $\zeta$ = -1

2x2 Gauss points are used for numerical integration.

## 3.6 Modeling of Laminated Shells

Modeling of laminated shells can be achieved by changing the numerical integration through thickness and constitutive equation. In this section the modification will be described.

### 3.6.1 Numerical Integration

The numerical integration is performed using the *Gauss quadrature* both in-plane and out-of -plane.The Gauss quadrature method approximates an integral as a summation over the evaluation points as follows:

$$\int_{-1}^{1}\int_{-1}^{1}\int_{-1}^{1} f(\xi,\eta,\zeta)\,|J|\,dr\,ds\,dt = \sum_{i,j,k} f(\xi_i,\eta_j,\zeta_k)\,|J|\,w_i w_j w_k \qquad (3.21)$$

The evaluation points, $\xi$ , $\eta$ and $\zeta$ are located symmetrically around the midpoint of the integration interval, and symmetrically paired evaluation points have the same weight factor, It has been shown by Gauss that the location of the evaluation points is determined as roots in the Legendre polynomial, Bathe (1996) [6]. Furthermore the expression in (3.21) is obtained by successive use of a one dimensional quadrature in each of the directions $\xi$ , $\eta$ and $\zeta$. Tabulations of Gauss-point locations and Gauss weight factors can be found in Bathe (1996) [6]. When Gauss quadrature is used in two or three dimensions it is most common to use the same order of integration in all directions, but different orders may be used in

different directions.

### 3.6.2 Numerical Thickness Integration of Laminates

For plane elements the through-the-thickness integration is normally performed explicitly by multiplying by the thickness of the element which is valid since both the strain-displacement matrix, B, and the jacobian matrix, J, are independent of the thickness coordinate, t. Consequently, they integrate as constants with regard to the thickness, i.e. $\int B\, dh = Bh$ where h is the shell thickness. In the present element formulation, the through-the-thickness integration cannot be performed explicitly since both the strain-displacement matrix and the Jacobian matrix are dependent on the thickness coordinate as shown in Equation (3.5) and Equation (3.13). Therefore integration in the thickness direction is performed numerically using the Gauss quadrature method in Equation (3.21). For laminated elements the thickness integration cannot be performed through the application of Equation (3.21) alone as explained in the following.

For laminated elements, where the material has orthotropic properties, different couplings such as extension-bending, extension-shear, shear-bending are introduced when the structure is not loaded in the principal material directions as discussed in Chapter 2. The behavior resulting from these coupling effects depends on the stacking sequence of the layers, the fiber orientation in the layers and the loading conditions. If the integration in the transverse direction is performed as one integration as for isotropic

shells the coupling effects will not be correctly included in the governing equations. Thus, the response of the model would not correlate with the response of the real structure.

The new integration scheme is set up as a *piecewise through-the-thickness* numerical integration, which seems natural when considering a laminated element as shown Figure (3.3).

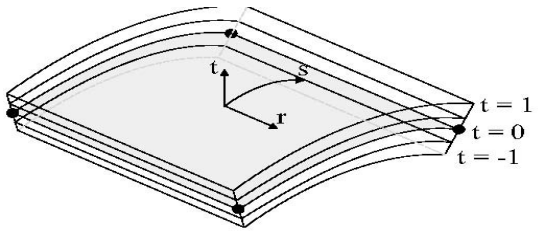


**Figure 3.15** A laminated element shown with four layers of equal thickness.

The constitutive matrix [C] will in general be different for each layer and in effect vary as a function of the thickness in global terms as explained in Section 3.7.

This property constitutes the fundamental problem of finding the constitutive matrix for an entire laminate. In classical laminate theory this problem is solved by using resultant formulation and dividing [C] into several matrices (the A-B-D approach described in Chapter 2). In the present study the integration of the laminated element is instead performed as a full three dimensional integration in each layer, meaning integration is performed over $\xi$, $\eta$ and $\zeta$ for all layers. Consequently, the individual layers are treated as "sub-elements" of the laminated element and thus, the stiffness of the entire element is determined as the sum of the layer stiffness contributions. By performing the integration of each layer separately in this manner the integration limits for the thickness

integration will be dependent on the set-up of the laminate (number of layers and layer thicknesses). Hence, to use the Gauss quadrature coefficients the integration limits have to be changed since integration must be carried out over the interval [−1; 1] when using Gauss quadrature. This is solved by transforming the transverse coordinate t into $t_l$ so that $t_l$ in the l'th layer varies from −1 to 1. This approach is shown in Figure( 3.4).

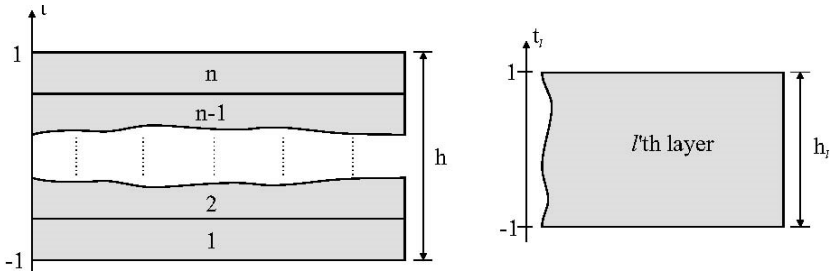


(a) (b)

Fig 3.4 Schematic representation of the integration scheme for laminated elements where (a) shows the entire element and (b) the l'th sub-layer where the transformed coordinate $t_l$ runs from −1 to 1.

The transformation of the natural coordinate, t, to a *layer coordinate*, $t_l$, is performed through the transformation

$$t = -1 + \frac{1}{h}(2\sum_{i=1}^{l} h_i - h_l(1-t_l)) \qquad (3.22)$$

where $h_l$ is the thickness of the l'th layer and the sum of the first term of the parenthesis constitutes the total thickness of the "preceding sub-elements". Inserting the modified coordinate in the Gauss integration represents integration by substitution and consequently, the derivative of the coordinate transformation in Equation (3.22) must be found and multiplied by the integrand. The derivative of Equation (3.22) is found as:

$$\frac{dl(t_l)}{dt_l} = \frac{h_l}{h} \Rightarrow dt = \frac{h_l}{h} dt_l \qquad (3.23)$$

The Gauss quadrature for laminated elements is thus stated as:

$$\int_{-1}^{1}\int_{-1}^{1}\int_{-1}^{1} f(\xi,\eta,\zeta)\left|J\right| dr\, ds\, dt_l = \sum_{i,j,k} f(\zeta_i,\eta_j,\zeta_k)\,\frac{h_l}{h}\left|J\right| w_i\, w_j w_k \qquad (3.24)$$

where $t_k$ is found from Equation (3.22). It can be clearly seen that the piecewise through-the-thickness integration of laminated elements makes them computationally expensive and hence, a lot of research has been made on how to increase the effectiveness of the integration. In Kumar and Palaninathan [21] different improved integration schemes for the piecewise through-the-thickness integration is discussed but none of these improved schemes have been implemented for the laminated shell elements presented here.

In principle the element formulation is completely described from the preceding sections. However, the resulting element (a so-called *purely displacement-based element*) will suffer heavily from locking, which is described and addressed in the following.

### 3.6.3 Constitutive Relation

Stresses are related to strains and hence displacements through a constitutive relation which for linear material behavior is Hooke's general law. In index notation this constitutive relation may be expressed generally by noting from the outer product rule that two second-order tensors can be related through a fourth-order tensor as:

$$\sigma_{ij} = c_{ijkl}\varepsilon_{kl} \qquad (3.25)$$

where the elastic coefficient tensor (or constitutive matrix in algebraic notation), $c_{ijkl}$,is to be determined. If the material considered is heterogenous the elastic coefficient tensor, $c_{ijkl}$, is dependent on the position and the elements of the tensor will be functions of the coordinates, $x_i$. However, since homogeneity is assumed for all materials

under investigation, $c_{ijkl}$, is independent of the position and the elements of the tensor are scalars. Consequently, since a fourth order tensor consists of $3^4$ =81 components, 81 equations in 81 unknowns must generally be solved to determine the relation in (3.26). However, applying various symmetry considerations, Timoshenko and Goodier [13] the relation in (3.26) can be reduced to an equation of 21 unknowns.

$$\begin{Bmatrix} \sigma_{11} \\ \sigma_{22} \\ \sigma_{33} \\ \sigma_{13} \\ \sigma_{23} \\ \sigma_{12} \end{Bmatrix} = \begin{bmatrix} c_{11} & c_{12} & c_{13} & c_{14} & c_{15} & c_{16} \\ & c_{22} & c_{23} & c_{24} & c_{25} & c_{26} \\ & & c_{33} & c_{34} & c_{35} & c_{36} \\ & & & c_{44} & c_{45} & c_{46} \\ sym. & & & & c_{55} & c_{56} \\ & & & & & c_{66} \end{bmatrix} \begin{Bmatrix} \varepsilon_{11} \\ \varepsilon_{22} \\ \varepsilon_{33} \\ \varepsilon_{12} \\ \varepsilon_{23} \\ \varepsilon_{13} \end{Bmatrix} \qquad (3.26)$$

This is the most general form of the so-called constitutive matrix, [C]. By assuming isotropic or orthotropic material behavior the number of constants in (3.26) can be further reduced.

In degenerated elements the constitutive relation is used not only to describe the material behavior but also for enforcing the Mindlin shell assumption of negligible transverse effects. As explained briefly earlier one of the Mindlin assumptions states that the mid-plane normal is in-extensible, i.e. there is no transverse normal strain, i.e. $\sigma_{33} = 0$, furthermore; it was assumed that the transverse normal stress is zero since the shell is thin to moderately thick. However, using the "full" constitutive relations would lead to transverse normal stresses due to

Poisson effects. This problem can be circumvented by forcing $\sigma_{33} = 0$ in the constitutive relation is demonstrated in the following:

First, an expression for the transverse normal stress is obtained, $\sigma_3 = 0$, by writing out the product of the strain vector and the third row of the constitutive matrix in Equation (3.26) as:

$$\sigma_3 = c_{31}\varepsilon + c_{32}\varepsilon_2 + c_{33}\varepsilon_3 + c_{34}\varepsilon_4 + c_{31}\varepsilon + c_{35}\varepsilon_5 + c_{36}\varepsilon_6 = 0 \qquad (3.27)$$

From Equation (3.27) the transverse normal strain can be isolated, yielding an expression for $\varepsilon_3$:

$$\varepsilon_3 = \frac{-c_{3i}\varepsilon_i}{c_{33}} \qquad (3.28)$$

where i=1,2,3,4,5,6. Inserting Equation (3.28) in the constitutive relation Equation (3.27) results in the following expression for the coefficients in modified constitutive matrix, [C]:

$$c_{ij}^{\ m} = c_{ij-}\frac{c_{i3}c_{3j}}{c_{33}} \qquad (3.29)$$

Where i=1,2,3,4,5,6 and j=1,2,4,5,6. Using Equation (3.29) on the **orthotropic** constitutive matrix Equation (3.26) yields the following matrix:

$$[c]^{\text{mod}} = \begin{bmatrix} c_{11} & c_{12} & 0 & 0 & 0 & 0 \\ & c_{22} & 0 & 0 & 0 & 0 \\ & & 0 & 0 & 0 & 0 \\ & & & c_{44} & 0 & 0 \\ \textit{symm.} & & & & c_{55} & 0 \\ & & & & & c_{66} \end{bmatrix} \qquad (3.30)$$

where the coefficients $c_{ij}$ are given as:

$$c_{11} = \frac{E_1}{1 - \nu_{12}\nu_{21}} \qquad c_{22} = \frac{E_2}{1 - \nu_{12}\nu_{21}} \qquad c_{11} = \frac{\nu_{21}E_1}{1 - \nu_{12}\nu_{21}} \tag{3.31}$$

$$c_{44} = G_{12} \qquad c_{55} = G_{23} \qquad c_{66} = G_{13}$$

Similar derivations can be made for the **isotropic** constitutive relation whereby the coefficients in the matrix in Equation (3.30) are given as:

$$c_{11} = c_{22} = \frac{E}{1 - \nu^2} \qquad c_{12} = \frac{\nu E}{1 - \nu^2} \qquad c_{44} = \frac{E}{2(1 + \nu)} \tag{3.32}$$

The coefficients in Equation (3.31) and Equation (3.32) are those used when formulating the constitutive relations for the shell elements since they contain the Mindlin assumption.

A further use of the constitutive relations is to correct the transverse shear stresses. If the transverse shear stresses are computed using three dimensional theory of elasticity, it can be shown that they will vary quadratic ally through the thickness. In order to obtain the same strain energy for the three dimensional solution and the shell element solution, the transverse shear stresses are corrected with the so-called *shear correction factor*, k, which is done by multiplying $C_{55}$ and $C_{66}$ with k.

The shear correction factor is not constant but dependent on geometry, the loading situation, the material properties and the boundary conditions as stated by Ochoa and Reddy (1992) [ 1]. In the isotropic case the factor does not change significantly and it is therefore common practice to use the factor obtained for a rectangular plate as done by. Zienkiewicz and Taylor [ 15 ], namely k=0.8. In the case of laminated structures the factor changes considerably when one or more of the aforementioned conditions are altered and consequently, it is necessary to recalculate the factor repeatedly. Several methods have been proposed for determining the correct factor. None of these methods have been implemented in the element formulation and the discussion will therefore not be extended further. Instead of calculating a shear correction factor for each laminated

structure considered, it is chosen to use k=0.8 for ordinary laminates and k=1.0 for sandwich shells.

The constitutive relation has now been fully developed but in order to use the matrix for determining k it must be transformed to the global coordinate system.

For **orthotropic** materials the constitutive matrix [C] in Equation (3.30) is dependent on orientation and by definition expressed in the principal material directions. Consequently, the transformation to the global coordinate system must be made from the principal material directions and not the lamina coordinate system. However, since both the transformation matrix T and the in-plane rotation of the material coordinate system are already defined it is convenient to use these transformations. To do so the transformation is carried out in one step presented blow:

$$[\mathbf{C}]^{\mathbf{mod}} = [\mathbf{T}]^{\mathbf{T}}[\mathbf{C}]\,[\mathbf{T}] \qquad (3.33)$$

where $[\mathbf{T}]$ is the transformation matrix given by

$$[\mathbf{T}] = \begin{bmatrix} a^2 & b^2 & 0 & 0 & 0 & 0 \\ b^2 & a^2 & 0 & 0 & 0 & 0 \\ 0 & 0 & 1 & 0 & 0 & 0 \\ -2ab & 2ab & 0 & a^2-b^2 & 0 & 0 \\ 0 & 0 & 0 & 0 & a & -b \\ b^2 & a^2 & 0 & 0 & b & a \end{bmatrix} \qquad (3.34)\ \text{a}$$

And

a and b are direction cosine given by

$$a = \cos(\theta) \qquad b = \sin(\theta) \qquad (3.34)\ \text{b}$$

This elaborates the statement made previously that almost all laminates will exhibit anisotropic behavior when loaded.

Using the constitutive matrix and the strain-displacement matrix

developed earlier we may assemble the element stiffness matrix by employing the expression $[K] = \int [B]^T [C] [B] dv$. For the sake of brevity the complete stiffness matrix is not stated. In order to assemble the stiffness matrix, which is an integral expression numerical integration must perform.

### 3.6.4 Mixed Interpolation of Tensorial Components – MITC

The MITC method is based on a change of strain component interpolations instead of a revised integration scheme as for selective (shear and bending terms integrated differently) integration. Consequently, the MITC approach uses full integration for all strain components but a new set of interpolation expressions. The MITC method was originally proposed for bilinear elements with a new transverse shear interpolation (the MITC4 element formulated by Dvorkin and Bathe [28] for eliminating shear locking), but has later been extended to higher order elements by Bucalem and Bathe [24]. This has lead to the MITC n-family of elements including triangular and quadrilateral elements with n number of nodes as suggested by Bucalem and Bathe [24], in which new interpolations are used for all strain components in order to simultaneously circumvent the problems of shear and membrane locking.

In general the "new" assumed strains (AS) will be expressed from the "old" or "directly interpolated" (DI) strains through a new set of interpolation functions as:

$$\tilde{\varepsilon}_{ij}^{AS} = \sum_{k=i}^{p} N_k^{ij}(r,s)\,\tilde{\varepsilon}_{ij}^{DI}(r_p, s_p, t) \qquad (3.35)$$

where $N_k^{ij}$ are the new interpolation functions in r and s corresponding to the ij'th strain and the k' th tying point. Note that the directly interpolated

strains in (3.35) constitute those calculated from a standard finite element formulation as the derivatives of the displacements. The new interpolations must naturally fulfill the relation:

$$N_k^{ij} \Big|^l \equiv N_k^{ij}(r_l, s_l) = \delta_{kl} \tag{3.36}$$

so that the k'th interpolation function assumes the value 1 in the k'th tying point and the value 0 in all other tying points. The new interpolations will generally be of the same order as the standard isoparametric interpolation functions used in the element, i.e. in the case of the bilinear element we use linear interpolations for the assumed strains.

The expression in (3.35) is the key assumption of the MITC method. The crucial point for the success of the method is the choice of *tying points*, $(r_p, s_p, t)$, from which the strains are interpolated. The tying points are chosen in the reference plane and the t-coordinate thus remains independent. It follows from (3.35) that the assumed strains and the directly interpolated strains are equal at the tying points. The location of the tying points in the natural coordinate system is given by Bathe and Dvorkin and Bathe [28] for most types of MITC elements. The rustication of the tying point coordinates is not given as a continuum mechanical explanation but is based on a numerical verification and the same approach will be taken here. In the following the derivation of the MITC interpolation expressions will be limited to the 4-node bilinear element; for this case the tying point are given by Bathe as in Figure(

3.5)

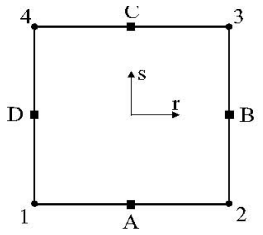


**Figure 3.18** Location of tying points for a MITC4 element; $A = (0,-1)$, $B = (1,0)$, $C = (0,1)$ and $D = (-1,0)$ in natural coordinates

The tying points, A and C, in Figure 3.5 are used for the interpolation of $\tilde{\varepsilon}_{13}$ and the points, B and D, are used for $\tilde{\varepsilon}_{23}$ and hence, the number of tying points, p, "per strain" is 2. The superscript assumed strain "AS" will be omitted in the following and it will be understood that the transverse shear strains are the new, interpolated strains.

To derive the interpolation expressions for the MITC4 element (3.35) is rewritten for a 4-node element by defining a new set of interpolation functions. Using the relation (3.36) a new set of linear interpolation functions for the four tying points are written tentatively as:

$$N_A^{13} = \frac{1}{2}(1-s) \qquad N_C^{13} = \frac{1}{2}(1+s) \tag{3.37 a}$$

$$N_B^{23} = \frac{1}{2}(1+r) \qquad N_D^{23} = \frac{1}{2}(1-r) \tag{3.37 b}$$

Using the interpolations of (3.35) in the general MITC expression (3.36) yields the new assumed strains:

$$\tilde{\varepsilon}_{13} = \frac{1}{2}(1-s)\,\tilde{\varepsilon}_{13}^{A} + \frac{1}{2}(1+s)\,\tilde{\varepsilon}_{13}^{C} \tag{3.38 a}$$

$$\tilde{\varepsilon}_{23} = \frac{1}{2}(1-r)\,\tilde{\varepsilon}_{23}^{D} + \frac{1}{2}(1+r)\,\tilde{\varepsilon}_{23}^{B} \tag{3.38 b}$$

This corresponds to a linear interpolation between the directly interpolated strains at points A−C and D−B, respectively. The directly

interpolated transverse strains are thus replaced by two assumed strains expressed in natural coordinates. To form the strain-displacement matrix these local strains must be transformed to global coordinates as described in Heinbockel . This is done using the standard tensor transformation:

$$\varepsilon_{ij} = \tilde{\varepsilon}_{kl}(g^k e_i)(g^l e_j) \tag{3.39}$$

where $e_i$ are the global base vectors. For the special case of plate, most of the terms in Equation (3.39) vanish but for the general case all nine components contribute to the global strain. The new strain-displacement matrix which incorporates the MITC method can be derived in a straight-forward.

## CHAPTER FOUR

# Geometrically Non-linear Finite Element Analysis

## 4.1 Introduction

In linear analysis it has been assumed that the geometry of the structure remains basically unchanged during the loading process, but the situation is different for nonlinear problems and large deformation may occur and as a consequence load–deformation curve is nonlinear. Therefore if accurate determination of displacements is needed, geometric non-linear analysis has to be performed. An important point must be mentioned that while linear problems have a unique solution non-linear problems may have more than one solution.

The earliest non-linear finite element analysis can be considered as an extension of linear one .

Two different approaches are adopted in incremental non-linear finite element analysis. The first approach is called updated Lagrangian approach in which all static and kinematic variables are referred to an updated configuration in each load increment. The second approach is

called total Lagrangian approach in which all static and kinematic variables are referred to the initial configuration.

Both Green's strains and geometric strains are used with 2nd Piola-Kirhhchoff stresses and engineering stresses respectively.

## 4.2 The Basic Problem

The general equilibrium equation for non-linear analysis can be written as

$$\psi(\mathbf{a}) = \int_{v} \bar{\mathbf{B}}^{T} \boldsymbol{\sigma}\, dv - \mathbf{f} = P(\mathbf{a}) - \mathbf{f} = 0 \qquad (4.1)$$

where;

$\psi$ = residual force

$\mathbf{f}$ = external force vector

$\mathbf{a}$ = nodal displacements

P = internal forces

$\bar{\mathbf{B}}$ is defined from the strain definition as

$$\boldsymbol{\delta\varepsilon} = \bar{\mathbf{B}}\ \delta\mathbf{a} \qquad (4.2)$$

and can be written as:

$$\bar{\mathbf{B}} = \mathbf{B}_O + \mathbf{B}_L(\mathbf{a}) \qquad (4.3)$$

And the strain

$$\varepsilon = \varepsilon_{\mathbf{o}} + \varepsilon_{\mathbf{L}} \qquad (4.4)$$

The stress strain relation remain as in linear analysis [2], thus

$$\sigma = C\varepsilon \qquad (4.5)$$

## 4.3 Solution Process

where the elastic coefficient tensor (or constitutive matrix in algebraic

notation), $c_{ijkl}$,is to be determined. If the material considered is heterogenous the elastic coefficient tensor, $c_{ijkl}$, is dependent on the position and the elements of the tensor will be functions of the coordinates, $x_i$. However, since homogeneity is assumed for all materials under investigation, $c_{ijkl}$, is independent of the position and the elements of the tensor are scalars. Consequently, since a fourth order tensor consists of $3^4$ =81 components, 81 equations in 81 unknowns must generally be solved to determine the relation in (3.26). However, applying various symmetry considerations Timoshenko and Goodier (1970) [ ] the relation in (3.26) can be reduced to an equation in 21 unknowns.

$$\delta\psi = \int_v \delta\overline{\mathbf{B}}^{\mathrm{T}}\boldsymbol{\sigma}\,d\upsilon + \int_v \overline{\mathbf{B}}^{\mathrm{T}}\delta\boldsymbol{\sigma}\,d\upsilon = \mathbf{K}_{\mathrm{T}}\,\delta\mathbf{a} \tag{4.6}$$

and using Equations (4.2) and (4.4) we have

$$\delta\boldsymbol{\sigma} = C\delta\boldsymbol{\varepsilon} = C\overline{\mathbf{B}}\ \delta\mathbf{a}$$

and if Equation(4.3 ) is valid

$$\delta\overline{\mathbf{B}} = \delta\mathbf{B}_L$$

Therefore

$$\delta\psi = \int_v \delta\mathbf{B}_L^T\sigma\,d\upsilon + \overline{\mathbf{K}}\,\delta\mathbf{a} \tag{4.7}$$

where

$$\overline{\mathbf{K}} = \int_v \overline{\mathbf{B}}^T C\overline{\mathbf{B}}\,d\upsilon = \mathbf{K}_O + \mathbf{K}_L \tag{4.8}$$

in which $\mathbf{K}_O$ represents the usual ,small displacements stiffness matrix, i.e.

$$\mathbf{K}_O = \int_v \mathbf{B}_O^T C \mathbf{B}_O \, d\upsilon \qquad (4.9)\ a$$

The matrix $\mathbf{K}_L$ is due to the large displacement and is given by

$$\mathbf{K}_L = \int_v (\mathbf{B}_O^T C \mathbf{B}_L + \mathbf{B}_L^T C \mathbf{B}_L + \mathbf{B}_L^T C \mathbf{B}_O) \, d\upsilon \qquad (4.9)\ b$$

$\mathbf{K}_L$: is variously known as the initial displacement matrix or large displacement matrix.

The first term of Equation (4.6) can generally be written as

$$\int_v \delta \mathbf{B}_L^T \sigma \, d\upsilon \equiv \mathbf{K}_\sigma \, \delta \mathbf{a} \qquad (4.10)$$

where $\mathbf{K}_\sigma$ is asymmetric matrix dependent on the stress level. This matrix is known as the initial stress matrix or geometric matrix. Thus:

$$\delta\psi = (\mathbf{K}_O + \mathbf{K}_\sigma + \mathbf{K}_L)\,\delta\mathbf{a} = \mathbf{K}_T \delta\mathbf{a} \qquad (4.11)$$

with $\mathbf{K}_T$ being the total, tangential stiffness matrix.

The steps followed in solution process are summarized as follows:

1-The elastic linear solution is obtained as first approximation $\mathbf{a}^o$.

2- The initial residual $\psi^o$ is found using Equation (4.1) with an appropriate definition of $\overline{\mathbf{B}}$ and stresses as given by Equation(4.4).

3- Matrix $\mathbf{K}_T^O$ is established.

4- Correction is computed as

$$\delta \mathbf{a}^o = -(\mathbf{K}_T^O)^{-1}\, \psi^O \qquad (4.12)$$

and steps 2,3 & 4 are repeated until $\psi^i$ becomes sufficiently small.

## 4.4 The Stress-strain Relations

The stress- strain relation is the same as that for linear analysis unless material non-linearity is considered

$$\boldsymbol{\sigma} = \mathbf{C}\boldsymbol{\varepsilon}$$

where $\boldsymbol{\sigma}$, $\mathbf{C}$ *and* $\boldsymbol{\varepsilon}$: are as defined previously.

## 4.5 Strain – displacement Relations

For three dimensions non-linear Green's strain-displacement relations are written as:

$$\varepsilon_x = \frac{\partial u}{\partial x} + \frac{1}{2}\left[\left(\frac{\partial u}{\partial x}\right)^2 + \left(\frac{\partial v}{\partial x}\right)^2 + \left(\frac{\partial w}{\partial x}\right)^2\right]$$

$$\gamma_{xy} = \frac{\partial u}{\partial y} + \frac{\partial v}{\partial x} + \left[\frac{\partial u}{\partial x}\frac{\partial u}{\partial y} + \frac{\partial v}{\partial x}\frac{\partial v}{\partial y} + \frac{\partial w}{\partial x}\frac{\partial w}{\partial y}\right] \qquad (4.13)$$

with other components obtained by suitable permutation as:

## 4.6 Derivation of $\mathbf{B}_L$ matrix

The general strain vector in three dimensions can be defined in terms of the infinitesimal and large displacement components

$$\boldsymbol{\varepsilon} = \boldsymbol{\varepsilon}_\mathbf{0} + \boldsymbol{\varepsilon}_\mathbf{L} \qquad (4.14)$$

$$\{\varepsilon_o\} = \begin{Bmatrix} \boldsymbol{\varepsilon}_x \\ \boldsymbol{\varepsilon}_y \\ \boldsymbol{\varepsilon}_z \\ \boldsymbol{\varepsilon}_{xy} \\ \boldsymbol{\varepsilon}_{xz} \\ \boldsymbol{\varepsilon}_{yz} \end{Bmatrix} = \begin{Bmatrix} \dfrac{\partial u}{\partial x} \\ \dfrac{\partial v}{\partial y} \\ \dfrac{\partial w}{\partial z} \\ \dfrac{\partial v}{\partial z} + \dfrac{\partial w}{\partial y} \\ \dfrac{\partial w}{\partial x} + \dfrac{\partial u}{\partial z} \\ \dfrac{\partial u}{\partial y} + \dfrac{\partial v}{\partial x} \end{Bmatrix} \qquad (4.15)$$

The non-linear term of Equation (4.10) can be conveniently rewritten as:

$$\boldsymbol{\varepsilon}_L = \frac{\mathbf{1}}{\mathbf{2}} \begin{bmatrix} \boldsymbol{\theta}_X^T & \mathbf{0} & \mathbf{0} \\ \mathbf{0} & \boldsymbol{\theta}_Y^T & \mathbf{0} \\ \mathbf{0} & \mathbf{0} & \boldsymbol{\theta}_Z^T \\ \mathbf{0} & \boldsymbol{\theta}_Z^T & \boldsymbol{\theta}_Y^T \\ \boldsymbol{\theta}_Z^T & \mathbf{0} & \boldsymbol{\theta}_X^T \\ \boldsymbol{\theta}_Y^T & \boldsymbol{\theta}_X^T \mathbf{0} & \mathbf{0} \end{bmatrix} \begin{Bmatrix} \boldsymbol{\theta}_X \\ \boldsymbol{\theta}_Y \\ \boldsymbol{\theta}_Z \end{Bmatrix} = \frac{\mathbf{1}}{\mathbf{2}} \mathbf{A}\,\boldsymbol{\theta} \qquad (4.16)$$

in which

$$\mathbf{A} = \begin{bmatrix} \boldsymbol{\theta}_X^T & \mathbf{0} & \mathbf{0} \\ \mathbf{0} & \boldsymbol{\theta}_Y^T & \mathbf{0} \\ \mathbf{0} & \mathbf{0} & \boldsymbol{\theta}_Z^T \\ \mathbf{0} & \boldsymbol{\theta}_Z^T & \boldsymbol{\theta}_Y^T \\ \boldsymbol{\theta}_Z^T & \mathbf{0} & \boldsymbol{\theta}_X^T \\ \boldsymbol{\theta}_Y^T & \boldsymbol{\theta}_X^T \mathbf{0} & \mathbf{0} \end{bmatrix}$$

and: $\boldsymbol{\theta}_x^T = \left[ \dfrac{\partial u}{\partial x}, \dfrac{\partial v}{\partial x}, \dfrac{\partial w}{\partial x} \right]$ etc.

hence:

$$\boldsymbol{\delta\varepsilon}_L = \frac{\mathbf{1}}{\mathbf{2}} \boldsymbol{\delta A}\ \boldsymbol{\theta} + \frac{\mathbf{1}}{\mathbf{2}} \mathbf{A}\boldsymbol{\delta\delta} = \mathbf{A}\ \boldsymbol{\delta\theta} \qquad (4.17)$$

and $\boldsymbol{\theta}$ can be determined in terms of the shape functions $N_i$ and nodal parameters $\mathbf{a}$ as :

$$\boldsymbol{\theta} = \mathbf{G}\mathbf{a} \tag{4.18}$$

or

$$\partial\boldsymbol{\varepsilon}_L = \mathbf{A}\mathbf{G}\delta\mathbf{a}$$

and

$$\mathbf{B}_L = \mathbf{A}\mathbf{G} \tag{4.19}$$

where

$$\mathbf{G} = \begin{bmatrix} \frac{\partial N_1}{\partial x} & \frac{\partial N_2}{\partial x}, & .... \\ \frac{\partial N_1}{\partial y} & \frac{\partial N_2}{\partial y} & .... \\ \frac{\partial N_1}{\partial z} & \frac{\partial N_2}{\partial z} & .... \end{bmatrix} \tag{4.20}$$

Thus $\mathbf{G}$ is matrix defined purely in terms of the coordinates.

## 4.7 Derivation of Tangent Stiffness Matrix $\mathbf{K}_T$

Noting that

$$\overline{\mathbf{B}} = \mathbf{B}_O + \mathbf{B}_L$$

We can form matrix $\overline{\mathbf{K}}$ such that

$$\overline{\mathbf{K}} = \mathbf{K}_0 + \mathbf{K}_L = \int_v \overline{\mathbf{B}}^T \mathbf{D}\, \overline{\mathbf{B}}\, \partial\upsilon \tag{4.21}$$

To complete the total tangential stiffness matrix it is necessary only to determine the initial stress matrix $\mathbf{K}_\sigma$. Again, by Equation (4.17) we have

$$\mathbf{K}_\sigma \delta\mathbf{a} = \int_v \delta\mathbf{B}_L^T \boldsymbol{\sigma}\, d\upsilon = \int_v \mathbf{G}^T \delta\mathbf{A}^T \sigma\, d\upsilon \tag{4.22}$$

Once again we can verify that we can write

$$\delta\mathbf{A}^T\boldsymbol{\sigma} = \begin{bmatrix} \sigma_X\mathbf{I}_3 & \tau_{XY}\mathbf{I}_3 & \tau_{XZ}\mathbf{I}_3 \\ & \sigma_Y\mathbf{I}_3 & \tau_{YZ}\mathbf{I}_3 \\ \text{Sym.} & & \sigma_Z\mathbf{I}_3 \end{bmatrix} \delta\boldsymbol{\theta} = \mathbf{M}\mathbf{G}\,\delta\mathbf{a} \tag{4.23}$$

in which $\mathbf{I}_3$ is 3x3 identity matrix.

Substituting Equation (4.20) into Equation (4.19) yields

$$\mathbf{K}_\sigma = \int_v \mathbf{G}^T\mathbf{M}\mathbf{G}\, d\upsilon \tag{4.24}$$

in which $\mathbf{M}$ is 9x9 matrix of the six 2nd Pilo – Kirchoff stress components arranged as in Equation (4.19).

Finally,

$$\mathbf{K}_T = \mathbf{K}_O + \mathbf{K}_L + \mathbf{K}_\sigma \tag{4.25}$$

**4.8 Geometrically Non-linear Formulation of Shell Element**

A total Lagrangian formulation based on Greens strains with 2nd Piola Kirchoff stresses and geometric strains with engineering stresses is presented in this section.

**4.8.1 Stresses and strains:**

For shell elements the stresses and strains are defined in a local coordinate system, say x,y,z. At any point axis z is normal to the surface ζ=constant, with the two other orthogonal axes x and y tangential to it. The Greens strains components and geometric strains components are given as follows:

for Green strains:

$$\{\varepsilon\} = \begin{Bmatrix} \varepsilon_x \\ \varepsilon_y \\ \gamma_{xy} \\ \gamma_{xz} \\ \gamma_{yz} \end{Bmatrix} \qquad (4.26)\ a$$

for geometric strains:

$$\{\varepsilon'\} = \begin{Bmatrix} \varepsilon_x' \\ \varepsilon_y' \\ \gamma_{xy}' \\ \gamma_{xz}' \\ \gamma_{yz}' \end{Bmatrix} \qquad (4.26)\ b$$

Considering the material to be linear elastic, the stresses corresponding to these strains are defined by:

for engineering stresses

$$\{\boldsymbol{\sigma}'\} = \begin{Bmatrix} \sigma'_x \\ \sigma'_y \\ \tau'_{xy} \\ \tau'_{xz} \\ \tau'_{yz} \end{Bmatrix} = [C]\ \{\boldsymbol{\varepsilon}'\} \qquad (4.27)\ a$$

for 2nd Piola stresses

$$\{\boldsymbol{\sigma}\} = \begin{Bmatrix} \sigma_x \\ \sigma_y \\ \tau_{xy} \\ \tau_{xz} \\ \tau_{yz} \end{Bmatrix} = [C]\{\boldsymbol{\varepsilon}\} \qquad (4.27)\ \text{b}$$

where $[C]$ is the elasticity matrix.

### 4.8.2 Strain – Displacement Relationship

**a) Green's strains**

Green's strains (including nonlinear terms) are given as:

$$\{\boldsymbol{\varepsilon}\} = \begin{Bmatrix} \varepsilon_x \\ \varepsilon_y \\ \gamma_{xy} \\ \gamma_{xz} \\ \gamma_{yz} \end{Bmatrix} = \begin{Bmatrix} \frac{\partial u}{\partial x} + \frac{1}{2}(\frac{\partial u}{\partial x})^2 + \frac{1}{2}(\frac{\partial y}{\partial x})^2 + \frac{1}{2}(\frac{\partial w}{\partial x})^2 \\ \frac{\partial v}{\partial y} + \frac{1}{2}(\frac{\partial u}{\partial y})^2 + \frac{1}{2}(\frac{\partial v}{\partial y})^2 + \frac{1}{2}(\frac{\partial w}{\partial y})^2 \\ \frac{\partial u}{\partial y} + \frac{\partial v}{\partial x} + \frac{\partial u}{\partial x}\frac{\partial u}{\partial y} + \frac{\partial v}{\partial x}\frac{\partial v}{\partial y} + \frac{\partial w}{\partial x}\frac{\partial w}{\partial y} \\ \frac{\partial u}{\partial z} + \frac{\partial w}{\partial x} + \frac{\partial u}{\partial x}\frac{\partial u}{\partial z} + \frac{\partial v}{\partial x}\frac{\partial v}{\partial z} + \frac{\partial w}{\partial x}\frac{\partial w}{\partial z} \\ \frac{\partial u}{\partial z} + \frac{\partial v}{\partial y} + \frac{\partial u}{\partial z}\frac{\partial u}{\partial y} + \frac{\partial v}{\partial z}\frac{\partial v}{\partial y} + \frac{\partial w}{\partial z}\frac{\partial w}{\partial y} \end{Bmatrix} \qquad (4.28)$$

Where $u, v$ and $w$ are the three components of the vector of displacements in the local co-ordinate system.

Equation (4.28) can be written in another form as follows:

$$\{\varepsilon\}=\begin{Bmatrix}\frac{\partial u}{\partial x}\\ \frac{\partial v}{\partial y}\\ \frac{\partial u}{\partial y}\frac{\partial v}{\partial x}\\ \frac{\partial u}{\partial z}\frac{\partial w}{\partial x}\\ \frac{\partial v}{\partial z}\frac{\partial w}{\partial y}\end{Bmatrix}+\frac{1}{2}\begin{bmatrix}\frac{\partial u}{\partial x} & \frac{\partial v}{\partial x} & \frac{\partial w}{\partial x} & 0 & 0 & 0 & 0 & 0 & 0\\ 0 & 0 & 0 & \frac{\partial u}{\partial y} & \frac{\partial v}{\partial y} & \frac{\partial w}{\partial y} & 0 & 0 & 0\\ \frac{\partial u}{\partial y} & \frac{\partial v}{\partial y} & \frac{\partial w}{\partial y} & \frac{\partial u}{\partial x} & \frac{\partial v}{\partial x} & \frac{\partial w}{\partial x} & 0 & 0 & 0\\ \frac{\partial u}{\partial z} & \frac{\partial v}{\partial z} & \frac{\partial w}{\partial z} & 0 & 0 & 0 & \frac{\partial u}{\partial x} & \frac{\partial v}{\partial x} & \frac{\partial w}{\partial x}\\ 0 & 0 & 0 & \frac{\partial u}{\partial z} & \frac{\partial v}{\partial z} & \frac{\partial w}{\partial z} & \frac{\partial u}{\partial y} & \frac{\partial v}{\partial y} & \frac{\partial w}{\partial y}\end{bmatrix}\begin{Bmatrix}\frac{\partial u}{\partial x}\\ \frac{\partial v}{\partial x}\\ \frac{\partial w}{\partial x}\\ \frac{\partial u}{\partial y}\\ \frac{\partial v}{\partial y}\\ \frac{\partial w}{\partial y}\\ \frac{\partial u}{\partial z}\\ \frac{\partial v}{\partial z}\\ \frac{\partial w}{\partial z}\end{Bmatrix} \qquad (4.29)a$$

Or

$$\{\boldsymbol{\varepsilon}\}=\{\boldsymbol{\varepsilon}_{\circ}\}+\{\boldsymbol{\varepsilon}_{\mathbf{L}}\}$$

where

$$\{\boldsymbol{\varepsilon}_{\circ}\}=[B_{\circ}]\{a\}$$

$$\{\boldsymbol{\varepsilon}_{\mathbf{L}}\}=\frac{1}{2}[A]\{\theta\} \qquad (4.29)\ b$$

$\{\boldsymbol{\varepsilon}_{\circ}\}$ are the strains for infinitesimal displacements

$\{\varepsilon_{\mathrm{L}}\}$ are the strains due to large displacements

$[B_{\circ}]$ is a matrix containing shape functions derivatives

$\{a\}$ is the vector of nodal displacements

Let:

$$[A]=\begin{bmatrix} \frac{\partial u}{\partial x} & \frac{\partial v}{\partial x} & \frac{\partial w}{\partial x} & 0 & 0 & 0 & 0 & 0 & 0 \\ 0 & 0 & 0 & \frac{\partial u}{\partial y} & \frac{\partial v}{\partial y} & \frac{\partial w}{\partial y} & 0 & 0 & 0 \\ \frac{\partial u}{\partial y} & \frac{\partial v}{\partial y} & \frac{\partial w}{\partial y} & \frac{\partial u}{\partial x} & \frac{\partial v}{\partial x} & \frac{\partial w}{\partial x} & 0 & 0 & 0 \\ \frac{\partial u}{\partial z} & \frac{\partial v}{\partial z} & \frac{\partial w}{\partial z} & 0 & 0 & 0 & \frac{\partial u}{\partial x} & \frac{\partial v}{\partial x} & \frac{\partial w}{\partial x} \\ 0 & 0 & 0 & \frac{\partial u}{\partial z} & \frac{\partial v}{\partial z} & \frac{\partial w}{\partial z} & \frac{\partial u}{\partial y} & \frac{\partial v}{\partial y} & \frac{\partial w}{\partial y} \end{bmatrix} \qquad (4.30)\text{ a}$$

and

$$\{\theta\}=\left\{\frac{\partial u}{\partial x} \quad \frac{\partial v}{\partial x} \quad \frac{\partial w}{\partial x} \quad \frac{\partial u}{\partial y} \quad \frac{\partial v}{\partial y} \quad \frac{\partial w}{\partial y} \quad \frac{\partial u}{\partial z} \quad \frac{\partial v}{\partial z} \quad \frac{\partial w}{\partial z}\right\}^{T}=[G]\{a\} \qquad (4.30)\text{ b}$$

where

$[G]$ is a matrix containing shape function derivatives.

$$[G]=\begin{bmatrix} \frac{\partial N_1}{\partial x} & 0 & 0 & 0 & 0 & ..... \\ 0 & \frac{\partial N_1}{\partial y} & 0 & 0 & 0 & ..... \\ 0 & 0 & \frac{\partial N_1}{\partial z} & 0 & 0 & ..... \\ \frac{\partial N_1}{\partial x} & 0 & 0 & 0 & 0 & ..... \\ 0 & \frac{\partial N_1}{\partial y} & 0 & 0 & 0 & ..... \\ 0 & 0 & \frac{\partial N_1}{\partial z} & 0 & 0 & ..... \\ \frac{\partial N_1}{\partial x} & 0 & 0 & 0 & 0 & ..... \\ 0 & \frac{\partial N_1}{\partial y} & 0 & 0 & 0 & ..... \\ 0 & 0 & \frac{\partial N_1}{\partial z} & 0 & 0 & ..... \end{bmatrix} \qquad (4.31)$$

$$\delta\{\boldsymbol{\varepsilon}_{\mathrm{L}}\}=\frac{1}{2}\delta[A]\{\theta\}+\frac{\mathbf{1}}{\mathbf{2}}[A]\delta\theta\{\theta\}=[A]\,\delta\{\theta\} \qquad (4.32)\text{a}$$

$$\delta\{\boldsymbol{\varepsilon}_{\mathrm{L}}\} = [A][G]\delta\{a\} = [B_{\mathrm{L}}]\delta\{a\}$$

Where,

$$[B_{\mathrm{L}}] = [A][G] \qquad (4.32)\text{b}$$

Also,

$$\delta\{\boldsymbol{\varepsilon}_{\circ}\} = [B_{\circ}]\delta a\{a\}$$

Then,

$$[B] = [B\circ] + [B_{\mathrm{L}}] \qquad (4.32)\text{c}$$

**b) Geometric strains**

According to the previous definition of the geometric strains

$$\varepsilon' = \begin{Bmatrix} \varepsilon_x' \\ \varepsilon_y' \\ \gamma_{xy}' \\ \gamma_{xz}' \\ \gamma_{yz}' \end{Bmatrix} = \begin{Bmatrix} (1+2\varepsilon_x)^{\frac{1}{2}} - 1 \\ (1+2\varepsilon_y)^{\frac{1}{2}} - 1 \\ \dfrac{\gamma_{xy}}{(1+2\varepsilon_x)^{\frac{1}{2}}(1+2\varepsilon y_y)^{\frac{1}{2}}} \\ \dfrac{\gamma_{xz}}{(1+2\varepsilon_x)^{\frac{1}{2}}} \\ \dfrac{\gamma_{yz}}{(1+2\varepsilon_y)^{\frac{1}{2}}} \end{Bmatrix} \qquad (4.33)$$

By taking the variation of Equation (4.30 ) we have:

$$\begin{Bmatrix} \delta\varepsilon_x' \\ \delta\varepsilon_y' \\ \delta\gamma_{xy}' \\ \delta\gamma_{xz}' \\ \delta\gamma_{yz}' \end{Bmatrix} = \begin{bmatrix} \frac{1}{(1+2\varepsilon_x)^{\frac{1}{2}}} & 0 & 0 & 0 & 0 \\ 0 & \frac{1}{(1+2\varepsilon_y)^{\frac{1}{2}}} & 0 & 0 & 0 \\ \frac{-\gamma_{xy}}{(1+2\varepsilon_x)^{\frac{1}{2}}(1+2\varepsilon_y)^{\frac{1}{2}}} & \frac{-\gamma_{xy}}{(1+2\varepsilon_x)^{\frac{1}{2}}(1+2\varepsilon_y)^{\frac{1}{2}}} & \frac{1}{(1+2\varepsilon_x)^{\frac{1}{2}}(1+2\varepsilon_y)^{\frac{1}{2}}} & 0 & 0 \\ \frac{-\gamma_{xy}}{(1+2\varepsilon_x)^{\frac{1}{2}}} & 0 & 0 & \frac{1}{(1+2\varepsilon_x)^{\frac{1}{2}}} & 0 \\ 0 & \frac{-\gamma_{yz}}{(1+2\varepsilon_y)^{\frac{1}{2}}} & 0 & 0 & \frac{1}{(1+2\varepsilon_y)^{\frac{1}{2}}} \end{bmatrix} \begin{Bmatrix} \delta\varepsilon_x \\ \delta\varepsilon_y \\ \delta\gamma_{xy} \\ \delta\gamma_{xz} \\ \delta\gamma_{yz} \end{Bmatrix}$$

(4.34)a

Or

$$\delta\{\varepsilon'\} = [H]\{\boldsymbol{\delta\varepsilon}\} \qquad (4.31b)$$

Subistitute equation (4.29b) into equation (4.31a)

$$\delta\{\varepsilon'\} = [H][B]\delta\{\varepsilon\} = [B^*]\delta\{a\} \qquad (4.34)b$$

$$[B^*] = [H][B]$$

and

$$[B] = [B\circ] + [B_L]$$

### 4.8.3 Tangent Stiffness Matrix due to Geometric Strains

The tangent stiffness matrix $[K_T]$ is obtained by differentiating the residual force vector $\{\psi\}$ with respect to the displacement vector $\{a\}$.

Where $\{\psi\}$ is given by:

$$\{\psi\} = \int_v [B^*]^T \{\sigma\} dv - f \qquad (4.35)$$

By differentiating equation with respect to $\{a\}$ , $[K_T]$ is obtained as:

$$\left\{\frac{\partial \psi}{\partial a}\right\} = [K_{\mathbf{T}}] = \int_{\mathbf{v}} [B]^{\mathbf{T}} [H]^{\mathbf{T}} \left\{\frac{\partial \sigma}{\partial a}\right\} d\mathbf{v} + \int_{\mathbf{v}} \frac{\partial [B]^{\mathbf{T}}}{\partial \{a\}} [H^{\mathbf{T}}] \{\sigma\} d\mathbf{v} + \int_{\mathbf{v}} [B]^{\mathbf{T}} \frac{\partial [H]^{\mathbf{T}}}{\partial \{a\}} \{\sigma\} dv$$

(4.34)

Using eq.(4.33) and eq.(4.34) gives:

$$\int_{\mathbf{v}} [B]^{\mathbf{T}} [H]^{\mathbf{T}} \left\{\frac{\partial \sigma}{\partial a}\right\} d\mathbf{v} = \int_{\mathbf{v}} [B]^{\mathbf{T}} [H\ ]^{T} [C][H][B] d\mathbf{v} = \int_{\mathbf{v}} [B^*]^{\mathbf{T}} [C][B^*] d\mathbf{v} = [K_{\circ}] + [K_{\mathbf{L}}]$$

(4.35) a

where

$$[K_{\circ}] = \int_{\mathbf{v}} [B_{\circ}]^{\mathbf{T}} [H]^{\mathbf{T}} [C] [H][B_{\circ}] dv \qquad (4.35)\ \text{b}$$

$$[K_{\mathbf{L}}] = \int_{\mathbf{v}} ([B_{\circ}]^{\mathbf{T}} [H]^{\mathbf{T}} [C][H][B_{\mathbf{L}}] + [B_{\mathbf{L}}]^{\mathbf{T}} [H]^{\mathbf{T}} [C][H][B_{\circ}] + [B_{\mathbf{L}}]^{\mathbf{T}} [H]^{\mathbf{T}} [C][H][B_{\mathbf{L}}]) dv$$

(4.35) c

From Equation (4.31a) and Equation (4.31b)

$$[H]^{T} \{\sigma\} = \{\sigma^*\} = \begin{Bmatrix} \sigma_x^* \\ \sigma_y^* \\ \tau_{xy}^* \\ \tau_{xz}^* \\ \tau_{yz}^* \end{Bmatrix} \qquad (4.36)$$

Using Equation (4.34) , Equation (4.36) and Equation (4.35) we can write:

$$\int_{\mathrm{v}} \frac{\partial [\mathrm{B}]^{\mathrm{T}}}{\partial \{\mathrm{a}\}} [\mathrm{H}]^{\mathrm{T}} \{\sigma\} \mathrm{dv} = \int_{\mathrm{v}} [\mathrm{G}]^{\mathrm{T}} [\mathrm{P}^*[\mathrm{G}] \mathrm{dv}] = [\mathrm{K}_{\sigma}] \qquad (4.37)$$

where:

$[K_\sigma]$ is the initial stress stiffness matrix

$[P^*]$ is the matrix of initial stress given by:

$$[P^*]=\begin{bmatrix} \sigma^*_X I_3 & \tau^*_{XY} I_3 & \tau^*_{XZ} I_3 \\ & \sigma^*_Y I_3 & \tau^*_{YZ} I_3 \\ Sym. & & 0 I_3 \end{bmatrix} \quad (4.38)$$

$I_3$ is 3x3 identity matrix

By differentiating Equation ( ) and using Equation ( ) and Equation ( ) the matrix $[K^*_T]$ is given as:

$$\int_v [B]^T \frac{\partial [H]^T}{\partial \{a\}} \{\sigma\} dv = \int_v [B]^T [P][B] dv = [K^*_\sigma] \quad (4.39)$$

where:

$[K^*_\sigma]$ is the additional geometric stiffness matrix

$[P]$ is the additional matrix of initial stress and is given in terms of the initial stresses and strains by:

$$[P]=\begin{bmatrix} \frac{-\sigma_x}{e_x^{\frac{1}{2}}}+\frac{3\gamma_{xy}\tau_{xy}}{e_x^{\frac{5}{2}}e_y^{\frac{1}{2}}}+\frac{3\gamma_{xz}\tau_{xz}}{e_x^{\frac{5}{2}}} & \frac{\gamma_{xy}\tau_{xy}}{e_x^{\frac{3}{2}}e_y^{\frac{3}{2}}} & \frac{-\tau_{xy}}{e_x^{\frac{3}{2}}e_y^{\frac{3}{2}}} & \frac{-\tau_{xy}}{e_x^{\frac{3}{2}}} & 0 \\ & \frac{-\sigma_y}{e_y^{\frac{1}{2}}}+\frac{3\gamma_{xy}\tau_{xy}}{e_x^{\frac{1}{2}}e_y^{\frac{5}{2}}}+\frac{3\gamma_{yz}\tau_{yz}}{e_x^{\frac{5}{2}}} & \frac{-\tau_{xy}}{e_x^{\frac{1}{2}}e_y^{\frac{3}{2}}} & 0 & \frac{-\tau_{yz}}{e_y^{\frac{3}{2}}} \\ & & 0 & 0 & 0 \\ symm. & & & 0 & 0 \\ & & & & 0 \end{bmatrix}$$

(4.40a)

where

$$e_x = (1+2\varepsilon_x)$$

and

$$e_y = (1+2\varepsilon_y) \quad (4.40b)$$

So tangent stiffness matrix due to geometric strains is given by:

$$[K_T] = [K_\circ] + [K_L] + [K_\sigma] + [K^*{}_\sigma] \tag{4.41}$$

### 4.8.4 Tangent Stiffness Matrix due to Green's Strains

The tangent matrix due to Green strains is obtained as follows:

$$\{\psi\} = \int_{\mathbf{v}} [B]^{\mathbf{T}} \{\sigma\} d\mathbf{v} - f \tag{4.42}$$

$$\left\{\frac{\partial \psi}{\partial a}\right\} = [K_T] = \int_v [B]^T \left\{\frac{\partial \sigma}{\partial a}\right\} dv + \int_v \frac{\partial [B]^T}{\partial \{a\}} \{\sigma\} dv \tag{4.43a}$$

$$\int_v [B]^T \left\{\frac{\partial \sigma}{\partial a}\right\} dv = \int_v [B]^T [D][B] dv = [K_\circ] + [K_L] \tag{4.43b}$$

In which

$$[K_\circ] = \int_v [B_\circ]^{T\,T} [D][B_\circ] dv \tag{4.43c}$$

$$[K_L] = \int_v ([B_\circ]^T [D][B_L] + [B_L]^T [D][B_\circ] + [B_L]^T [D][B_L]) dv \tag{4.43d}$$

Using eq.(4.43a) and eq.(4.43b)

$$\int_v \frac{\partial [B]^T}{\partial \{a\}} \{\sigma\} dv = \int_v [G]^T \frac{\partial [A]^T}{\partial \{a\}} \{\sigma\} dv = [K_\sigma] \tag{4.44a}$$

Once again we can write:

$$\frac{\partial [A]^T}{\partial \{a\}} \{\sigma\} = \begin{bmatrix} \sigma_x [I] & \tau_{xy} [I] & \tau_{xz} [I] \\ & \sigma_x [I] & \tau_{yz} [I] \\ symm. & & 0[I] \end{bmatrix} [G] = [M]_{9x9} [G] \tag{4.44b}$$

$$[I] = \begin{bmatrix} 1 & 0 & 0 \\ & 1 & 0 \\ symm. & & 1 \end{bmatrix} \tag{4.44c}$$

Substituting eq. into eq. yields:

$$[K_\sigma] = \int_v [G]^T [M][G]\, dv \qquad (4.44d)$$

By substituting Equation (4.44a) and Equation (4.44d) into Equation (4.42) the tangent stiffness matrix due to Greens strains is defined by:

$$[K_T] = [K_\circ] + [K_L] + [K_\sigma] \qquad (4.45)$$

The following chapter presents description of the computer program to be implemented for analyzing laminated shell structures.

# CHAPTER FIVE

# Description of the Computer Program

## 5.1 General:

A computer program named **NFEAP** (**N**onlinear **F**inite **E**lement **A**nalysis **P**rogram) written in standard **FORARAN 77** is described in this section. The program can be used to analyze structures:

1. Single layer and multilayer
2. Isotropic and orthotropic

3. Linear and nonlinear
4. Based on Green's strains or Geometric strains

Total Lagrangian Formulation is adopted.

Mesh generation scheme is developed in the program for cylindrical shell, spherical shell and flat plate. Other structures can be analyzed by inserting appropriate mesh generation in the program.

Eight points integration scheme is used also other integration scheme can easily be used by modifying the program.

The programs developed have the facility to use different material types.

The sign conventions adopted are as follows:

1- Anti-clockwise moments are positive.
2- Loads are considered positive when acting in the positive direction of the global axes.
3- Displacements are considered positive when nodes move towards positive direction of the global axes.

The main program flow chart and subroutines are shown in Figure (5.1).

Appendix I shows the main program code

Appendix II shows one sample of input file

Appendix III shows a portion of output data

Brief descriptions will be presented for the main program and each subroutine.

## 5.2 The Main Program

The main program, which controls the various tasks of the program, calls a number of subroutines and its organizational structure is indicated in flow chart presented in Fig. 5.1.

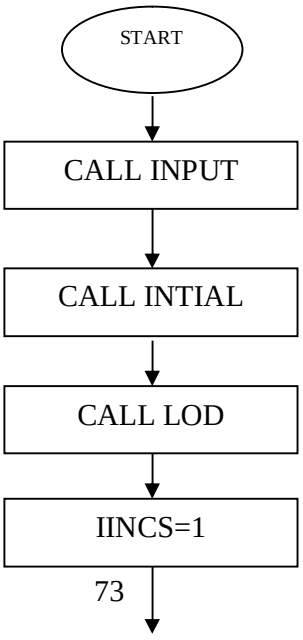
START
CALL INPUT
CALL INTIAL
CALL LOD
IINCS=1
73

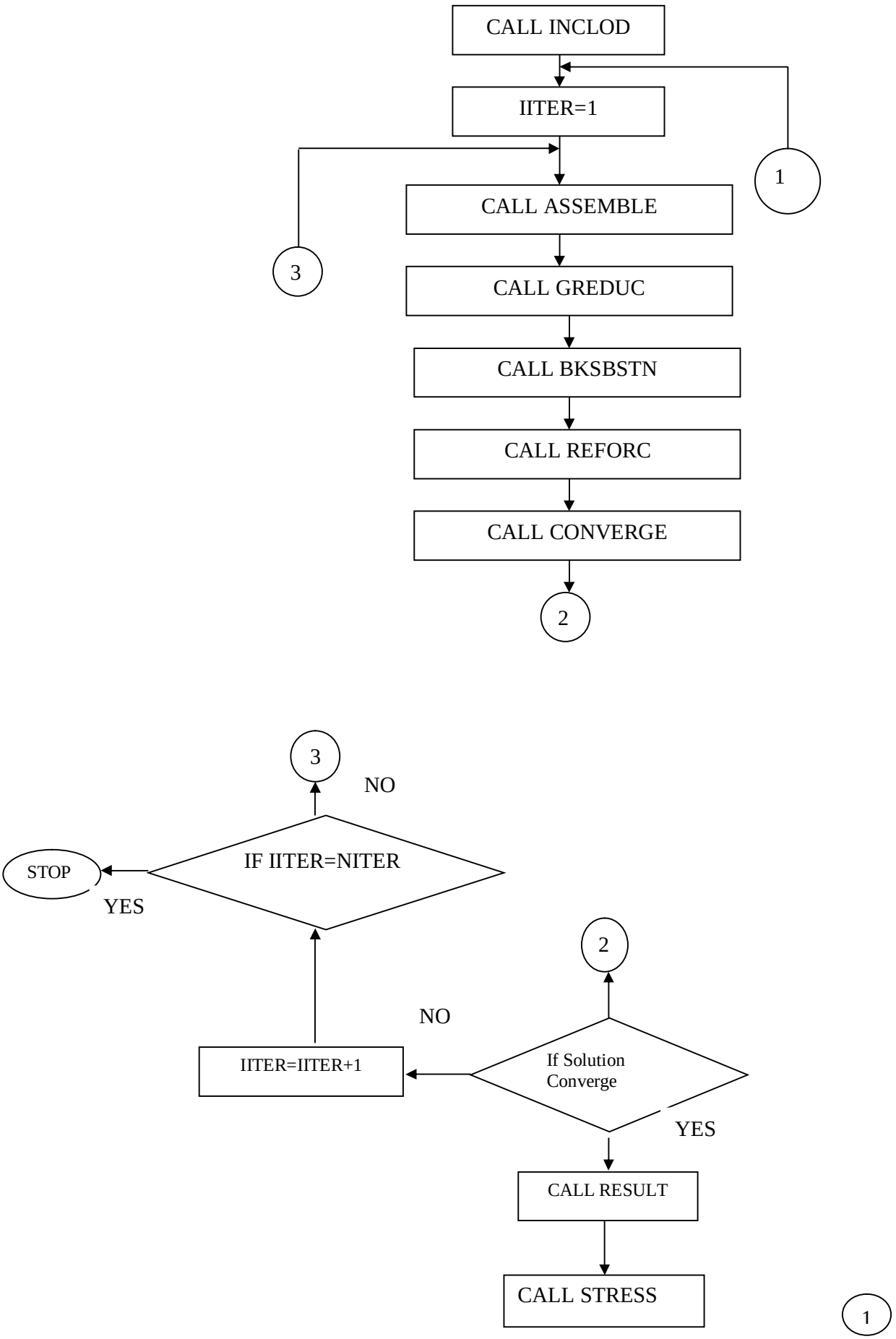
CALL INCLOD
IITER=1
1
CALL ASSEMBLE
3
CALL GREDUC
CALL BKSBSTN
CALL REFORC
CALL CONVERGE
2
3
NO
STOP
IF IITER=NITER
YES
2
NO
IITER=IITER+1
If Solution
Converge
YES
CALL RESULT
CALL STRESS
1

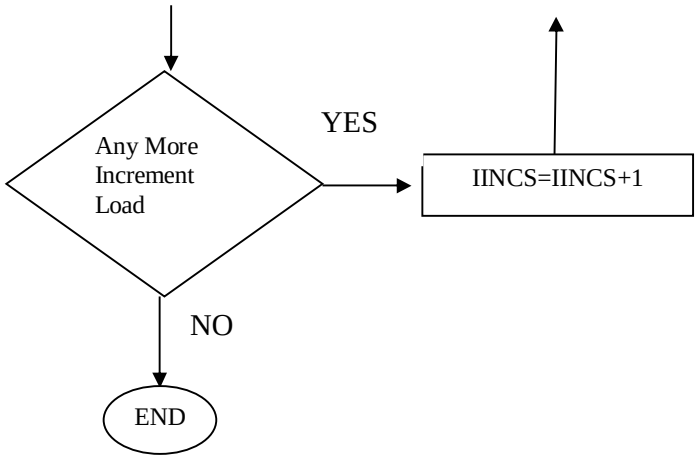


Figure (5.1) Main Program Flow Chart

## 5.3 Subroutine **INPUT**

The subroutine **INPUT** reads the necessary data that defines the structure geometry, properties of the elements, boundary conditions and elemental and nodal load. It also generates the element nodal connections and generates the co-ordinates of points.The subroutine **INPUT** reads data from the file called "**INDAT**". The reading is free format and separated by commas (,). The user is free to adopt any consistent system of units.

The details of writing the data in file "**INDAT"** are as follows:

5.3.1 Control and geometric data is presented as described in Table 5.1

Table 5.1 **CONTROL & GEOMETRIC DATA**

| **Variable** | **Description** |
|---|---|
| NBOUN | Number of boundary conditions |
| NELAC | Number of elements along curve |
| NELAH | Number of elements along straight line |
| NINCS | Number of load increments |
| ROUT | Outer radius |

| | |
|---|---|
| RIN | Inner radius |
| THICK | Thickness of element |
| NMATS | Number of material types |
| NNODE | Number of nodes per element [16] |
| NDOFN | Number of degrees of freedom per node [3] |
| NPROP | Number of properties [5] |
| HLENG | Length of straight line |
| ALPHA1 | Left angle in degrees calculated from horizontal to the beginning of curve |
| ALPHA1 | Right angle in degrees calculated from horizontal to the end of the |
| NGAUS | Number of Gauss points |
| NDIME | Number of dimensions |

5.3.2 Material property data is prepared as described in Table 5.2

Table 5.2 **MATERIAL PROPERTIES DATA**

| **Variable** | **Description** |
|---|---|
| JMATS | Property set number (1,…,number of material types) |
| PROPS(JMATS,1) | E , Young's modulus |
| PROPS(JMATS,2) | $\nu$, Poison's ratio |
| PROPS(JMATS,3) | $\rho$ , Density of the element material |
| PROPS(JMATS,4) | W , Uniform vertical load per unit area |
| PROPS(JMATS,5) | $P_n$ , Uniform surface pressure per unit area |

5.3.3 Co-ordinates data is prepared as described in Table 5.3

Table 5.3 **CO-ORDINATES DATA**

| Only the co-ordinates of point (1) must be input | |
|---|---|
| **Variable** | **Description** |
| COORD(1,1) | x-co-ordinate of point (1) |
| COORD(1,2) | y-co-ordinate of point (1) |
| COORD(1,3) | z-co-ordinate of point (1) |

5.3.4 Boundary restrained data is prepared as described in Table 5.4

Table 5.4 BOUNDARY CONDITIONS DATA

| For each point which has at least one degree of freedom with a specified displacement, a boundary condition must be input . The convention used for boundary restraints is :<br>ICODE,VALUE = 0,0 no restraints<br>( 1, value if restrained (value =0) or displacement specified (value = value of displacement). | |
|---|---|
| **Variable** | **Description** |

| | |
|---|---|
| NODFX | Point number |
| ICODE(1),VALUE(1) | For displacement at x-direction(u) |
| ICODE(2),VALUE(2) | For displacement at y-direction(v) |
| ICODE(3),VALUE(3) | For displacement at z-direction(z) |

5.3.5 Element properties data is prepared as described in Table 5.5

Table 5.5 **ELEMENT PROPERT IES DATA**

| The element data contains the element number and material set number | |
|---|---|
| **Variable** | **Description** |
| JELEMENT | Element number |
| MATNO(JELEM) | Material type number |

5.3. 6 Point load is input as described in Table 5.6

Table 5.6 **POINT LOAD DATA**

| For each point that has non-zero point load, a load record must be input | |
|---|---|
| **Variable** | **Description** |
| IPOIN | Point number |
| PLOAD(IPOIN,1) | Force in x-direction |
| PLOAD(IPOIN,2) | Force in y-direction |
| PLOAD(IPOIN,3) | Force in z-direction |

5.4 Subroutine **INITIAL**

This subroutine sets initial values for loads and displacements.

5.5 Subroutine **LOD**:

This subroutine calculates the equivalent joint load due to self-weight, vertical load and surface load. The summation of these loads with the addition of point loads are calculated and stored in **RLOAD** (**ISVAB**), (**ISVAB**=1,…, total number of structure variables ).

5.6 Subroutine **INCLOD**

This subroutine reads the factors of load increments, maximum number of iteration and tolerance.

The number of increments and the load factor values are free for the user's choice but the summation of factors must be equal to 1.

The prescribed values must be multiplied by the factor at each load increment so as to be compatible with load value.

5.7 Subroutine **ASSEMBLE**

The subroutine **LSTIFF** calculates the element stiffness matrix and stores it in **ESTIF** Figure (5.2). The subroutine **ASSEMBLE** calls this subroutine and sets the overall stiffness matrix in a column vector **ASTIFF (MSTIF), (MSTIF**=1,…, maximum value depends on the band width ).

5.8 Subroutine **GREDUC** and **BKSBSTN**

According to the Gauss elimination the subroutine **GREDUC** reduces the equations and the solution is completed by the subroutine **BKSBSTN**. The result of this solution is the displacements given by the vector **TDISP** (**ISVAB**). In addition reaction forces are also obtained.

5.9 Subroutine **REFORC**

This subroutine calculates the internal force given by the expression $\int_v \mathbf{B}^T \sigma \, dv$ for each element and stores it in **ELOAD (IELEM, IEVAB),** **(IELEM**=1… Number of element variables).

5.10 Subroutine **CONVERGES**:

This subroutine checks the convergence of the solution by checking the ratio of residual force to the external force, this ratio must be less than the tolerance. The tolerance takes a value between (0.1 - 1%).

5.11 Subroutine **RESULTS** & **STRES**

The subroutine **RESULT** prints out the displacements in (outdat2) file and subroutine **STRES** compute and print stresses.

5.12 Subroutine **DMATX:**

This subroutine calculates the constitutive equation elements. In case of orthotropic material we need to a transformation from material coordinates system to problem coordinate system.

The next chapter presents results of numerical examples that have been solved using this program together with comparison with known results.

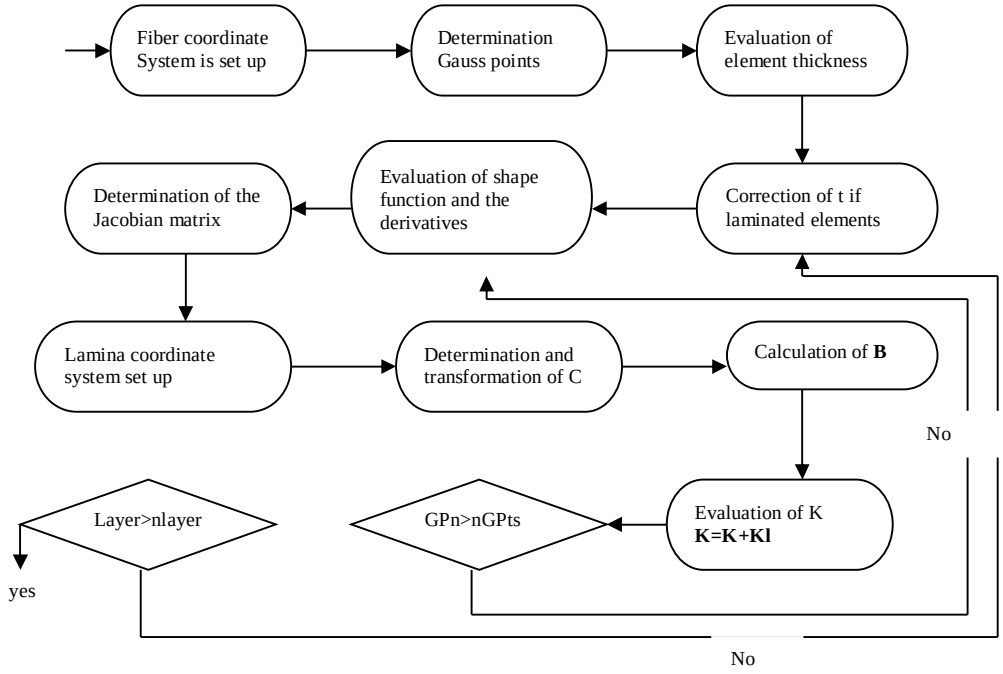


Figure (5.2) Schematic representation of the determination of the stiffness matrix

# CHAPTER SIX

# APPLICATION TO NUMERICAL EXAMPLES AND DISCUSSION OF RESULTS

The numerical examples discussed in this study comprise seven different shell structures namely: simply supported rectangular plate,orthotropic square plate,simply supported square plate under sinusoidal load, barrel vault, pinched cylinder, laminated cylindrical shell and doubly curved

shell. For each example the basic structural data is displayed with sketches. Analysis results are compared with published results is given in tabulated and graphical form.

## 6.1 Application to Numerical Examples

### 6.1.1 Convergence of displacement for simply supported plate:

The simply supported square plate shown in Figure (6.2) is loaded transversely with uniform pressure. Problem data is a=b=400 cm, $E=2x10^3$ KN/cm, thickness=12 cm, $q=5.88KN/m^{2.}$

A quarter of the plate is modeled with 1, 4, 8 and 16 eight node degenerated elements and vertical displacement of the plate is computed to assess the convergence of the finite element model by increasing the no of elements. Rapid convergence was observed as shown in Figure (6.1).

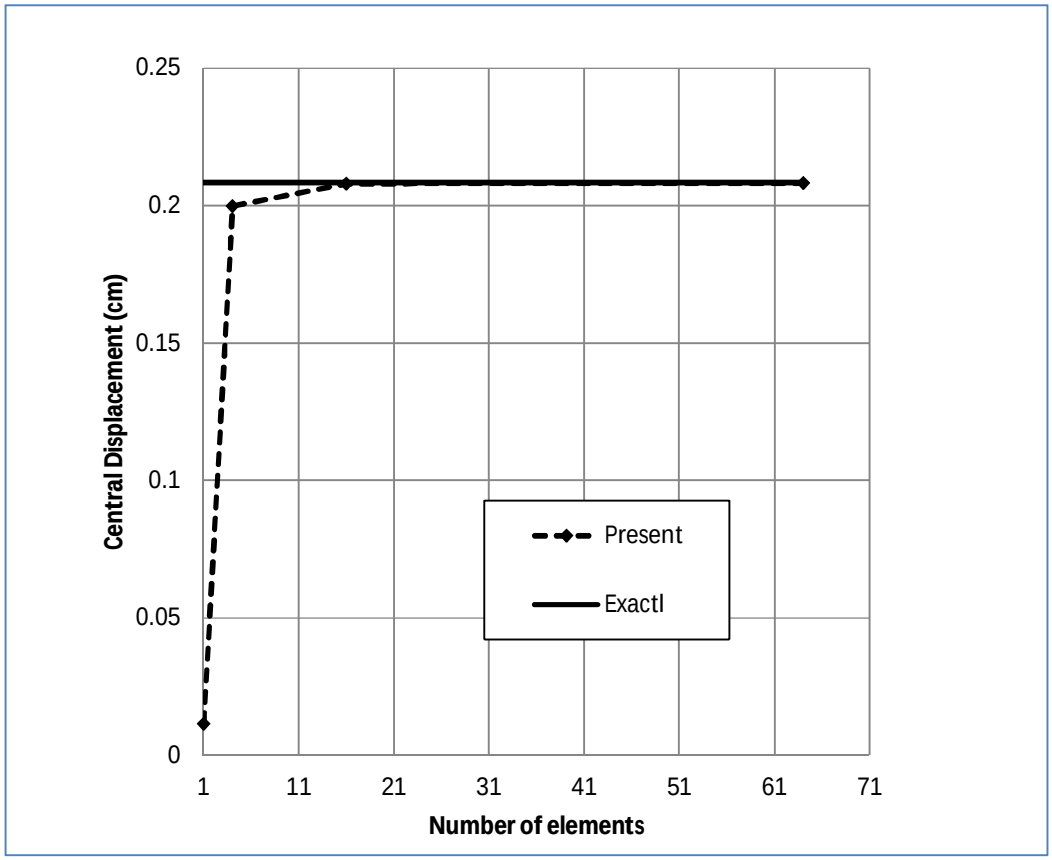


Figure (6.1) Convergence of Vertical Displacement

### 6.1.2 Orthotropic square plate under uniform load:

Here we consider a simply supported, orthotropic, square plate under uniform transverse load $\mathbf{q}_o$ is shown in Figure (6.2). The geometry and material parameters used here are

a=b=12 in., h=0.$_{138}$ in., $E_1=3x10^6$ psi, $E_2=1.28x10^6$ psi

$G_{12}=G_{13}=G_{23}=0.37x10^6$ psi, $\nu_{12}=0.25$

A quarter of the plate with simply supported boundary conditions and symmetry is modeled with 4x4 eight node elements. The present results shown in Figure (6.3) are in good agreement with experimental results of Zaghloul and Kennedy [26 ].

Table (6.1) presents numerical results obtained by using Green's and Geometric strain. The two results are approximately the same.

Tables (6.2) & (6.3) present a comparison of moments ($M_x$) at the centre of the plate and twisting moments ($M_{xy}$) at the corner of the plate. No significant difference is found between the two formulations.

Figure (6.4) shows a plot for the data presented in Table (6.2). It is observed that the difference percent in stresses is greater than that of displacements. The reason is that displacements are directly computed at Gauss points of integration and interpolated or extrapolated to the boundary nodes of the elements, but stresses are derived from displacements.

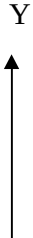

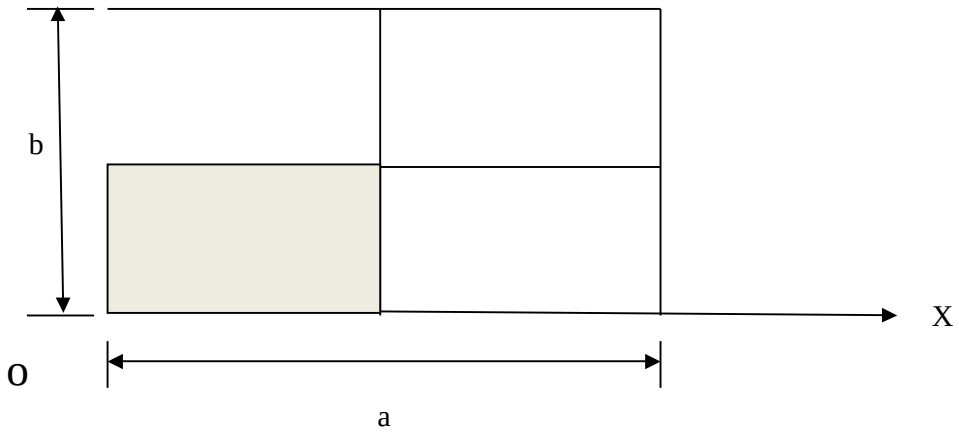


Figure (6.2) Simply square plate under uniform load

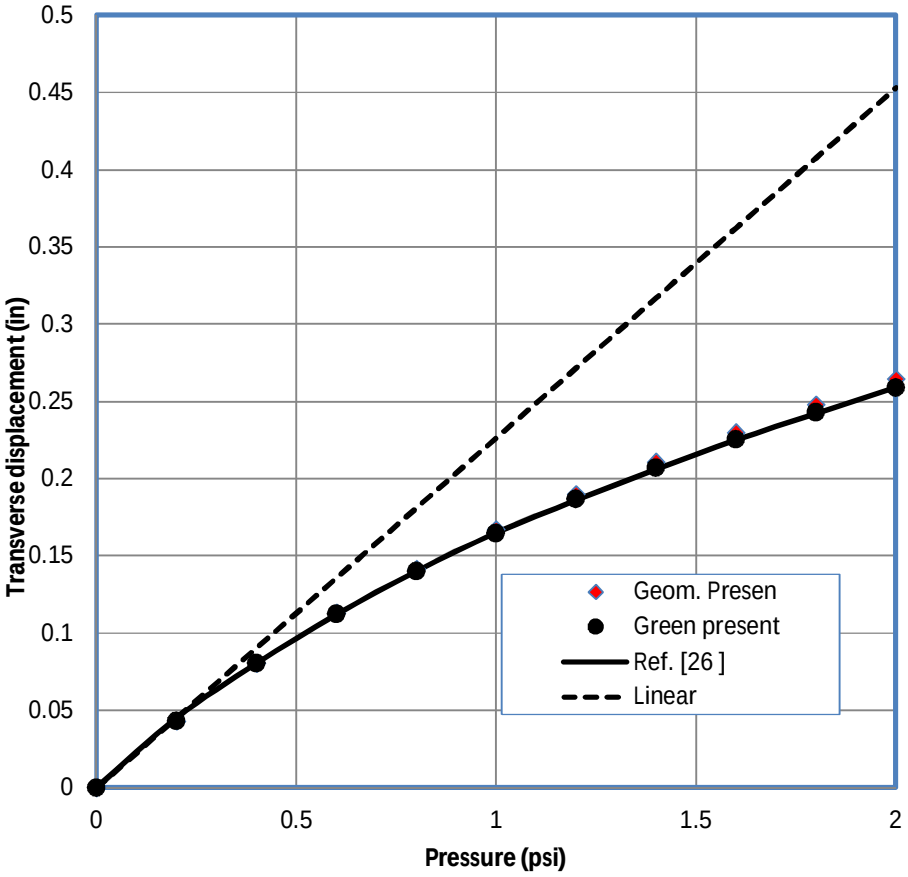


Figure (6.3) Transverse displacement vs. pressure load

Table (6.1) Comparison of displacements

| Inc. No. | Pressure (psi) | Green disp. (in.) | Geom. Disp. (in.) | Difference (%) |
|---|---|---|---|---|
| 1 | 0.2 | 0.04301 | 0.04301 | 0 |
| 2 | 0.4 | 0.08034 | 0.08060 | .3 |
| 3 | 0.6 | 0.11230 | 0.11318 | .8 |
| 4 | 0.8 | 0.14003 | 0.14175 | 1.2 |
| 5 | 1.0 | 0.16458 | 0.16717 | 1.6 |
| 6 | 1.2 | 0.18671 | 0.19007 | 1.8 |
| 7 | 1.4 | 0.20688 | 0.21094 | 2.0 |
| 8 | 1.6 | 0.22549 | 0.23016 | 2.1 |
| 9 | 1.8 | 0.24282 | 0.24800 | 2.1 |
| 10 | 2.0 | 0.25902 | 0.26467 | 2.2 |

Table (6.2) Comparison of moments ($10^3 \times M_x$) at the centre of the plate

| Incr. No. | Pressure(psi) | Green moments lb-in/in | Geom. Moments lb- in/in | Difference percent (%) |
|---|---|---|---|---|
| 1 | 0.1 | .218 | .218 | 0.0 |
| 2 | 0.2 | .401 | .399 | 0.5 |
| 3 | 0.3 | .551 | .545 | 1.1 |
| 4 | 0.4 | .676 | .665 | 1.6 |
| 5 | 0.5 | .782 | .765 | 2.2 |
| 6 | 0.6 | .874 | .852 | 2.5 |
| 7 | 0.7 | .954 | .928 | 2.7 |
| 8 | 0.8 | 1.025 | .995 | 2.9 |
| 9 | 0.9 | 1.088 | 1.055 | 3.0 |

| | | | | |
|---|---|---|---|---|
| 10 | 1.0 | 1.145 | 1.110 | 3.1 |

Table (6.3) Comparison of moments ($10^3 \times M_{XY}$) at the centre of the plate

| Incr. No. | Pressure(psi) | Green moments lb-in/in | Geom. Moments lb- in/in | Difference percent (%) |
|---|---|---|---|---|
| 1 | 0.1 | .058 | .058 | 0.0 |
| 2 | 0.2 | .112 | .112 | 0.0 |
| 3 | 0.3 | .163 | .163 | 0.0 |
| 4 | 0.4 | .211 | .210 | 0.5 |
| 5 | 0.5 | .258 | .256 | 0.8 |
| 6 | 0.6 | .302 | .300 | 0.7 |
| 7 | 0.7 | .346 | .343 | 0.9 |
| 8 | 0.8 | .388 | .385 | 0.8 |
| 9 | 0.9 | .430 | .426 | 9.3 |
| 10 | 1.0 | .470 | .466 | 0.9 |

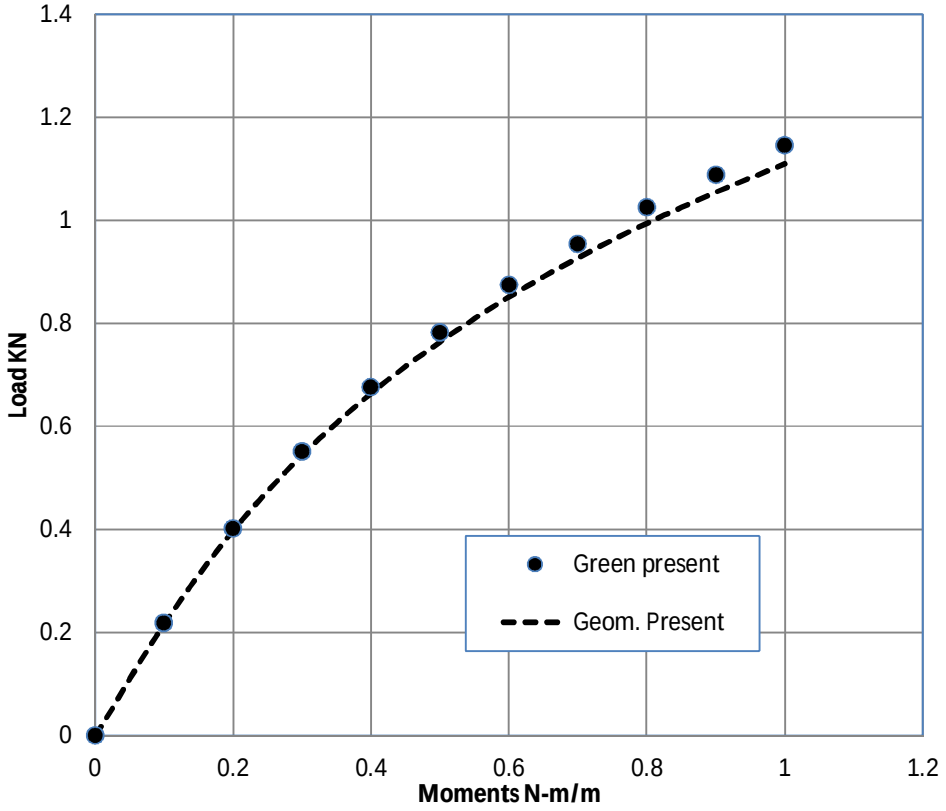


Figure (6.4) Load vs. Moments at the centre of the plate

### 6.1.3 Simply supported square laminated plate under sinusoidal load:

The simply supported square plate shown in Figure (6.2) is subjected to sinusoidal load. The lamination scheme is 0/90/90/0 degrees.

Table (6.2) contains the nondimensionalized deflections and stresses for different side –to-thickness ratios. ($E_1$=25$E_2$ ,$v_{12}$=0.25 , $G_{12}$=$G_{13}$=0.5$E_2$, $G_{23}$=0.2$E_2$ , $K$=5/6)

The following nondimensionalizations are used to present results in graphical and tabular form

$$\bar{w} = w_o \left(\frac{E_2\, h^3}{b^4\, q_o}\right) \qquad \bar{\sigma}_{xx} = \sigma_{xx} \left(\frac{h^2}{b^2\, q_o}\right)$$

$$\bar{\sigma}_{yy} = \sigma_{yy} \left(\frac{h^2}{b^2\, q_o}\right) \qquad \bar{\sigma}_{xy} = \sigma_{xy} \left(\frac{h^2}{b^2\, q_o}\right)$$

$$\bar{\sigma}_{xz} = \sigma_{xz} \left(\frac{h}{b\, q_o}\right) \qquad \bar{\sigma}_{yz} = \sigma_{yz} \left(\frac{h}{b\, q_o}\right)$$

Table (6.4) Deflections and Stresses vs. side-to –thickness ratio

| | *a/h* | Load | $\bar{w} \times 10^2$ | $\bar{\sigma}_{xx}$ | $\bar{\sigma}_{yy}$ | $\bar{\sigma}_{xxy}$ |
|---|---|---|---|---|---|---|
| Ref. [8] | 100 | SSL | 0.4337 | .0.5382 | 0.2704 | 0.0213 |
| Present | | | 0.4338 | 0.5520 | 0.2775 | 0.0219 |

Figure (6.5) shows a plotting for the deflections against modular ratios. It observed that the proposed mathematical model correlate very well with the analytical solution. In this model (y) represent the deflection and (x) represent modular ratio.

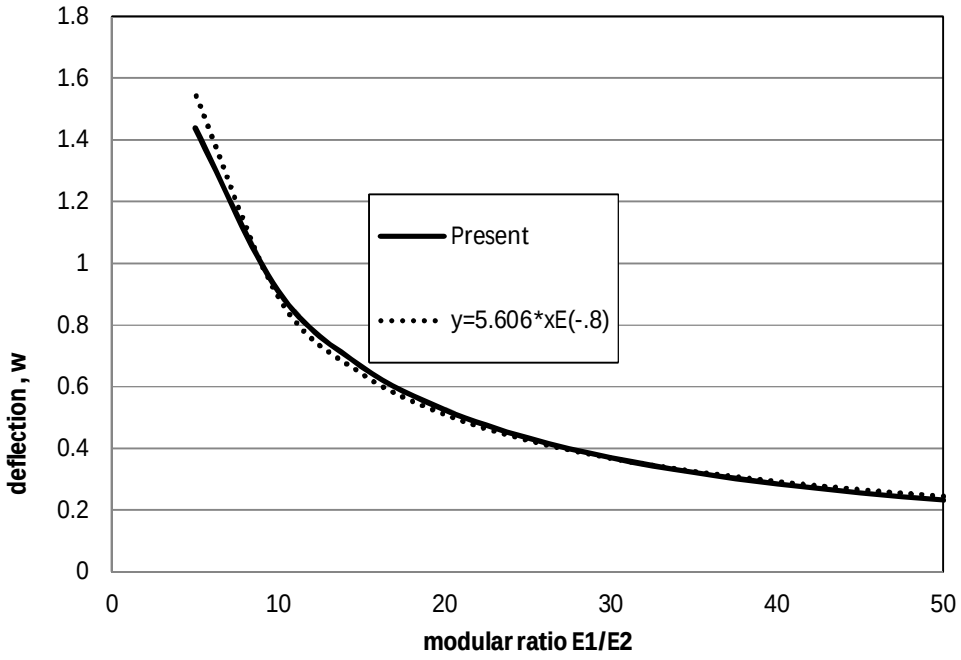


Figure (6.5) Modular ratios vs. central deflections

Figure (6.6) shows plot vertical deflections vs. different side – to – thickness ratio . The present solution converge to **FSDT**( first order shear deformation theory for side –to- thickness ratio of (100).

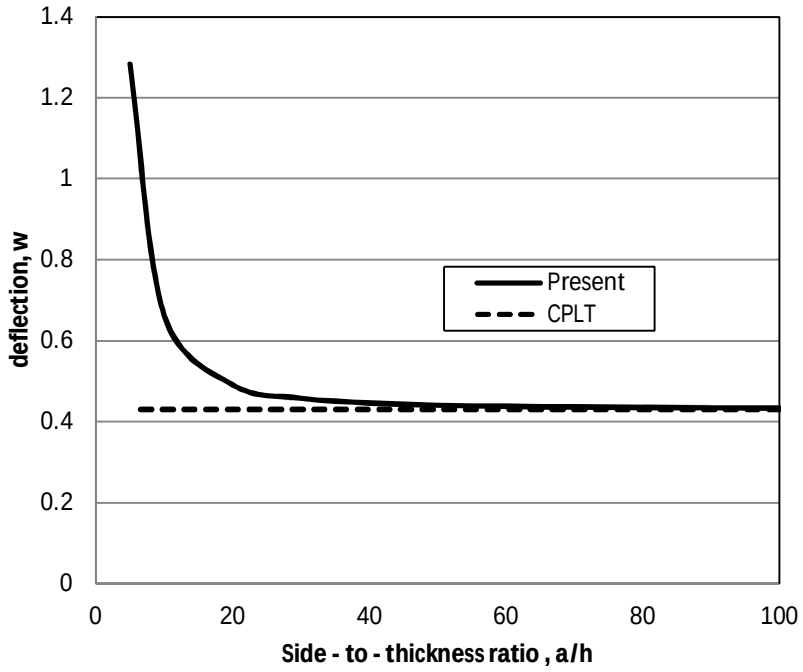


Figure (6.6) Vertical deflections vs. side-to-thickness ratio

### 6.1.4 Barrel vault:

This is a well known benchmark problem known as Scordelies-Lo roof. A solution to this problem was first discussed by Cantin and Clough [34] (who used $\nu$=0.3). The problem consists of a cylinder roof with rigid supports at edges x = ± a/2 while edges at y = ± b/2 are free. The shell is assumed to deform under its own weight (i.e., q acts vertically down, not perpendicular to the surface of the shell). The geometric and material data of the problem is (see Figure 6.7):

$\alpha$= 40˚ (0.698 radians), R=300 in., a=600 in., h=3 in., E=3x$10^6$ psi. $\nu$=0.0, q=0.625psi. The boundary conditions on the computational domain are

At x=0: v=$\beta$=0, At x=a/2: u=w=$\alpha$=0, At y=0: u= $\beta$=0, At y=b/2: Free.

A mesh of 4x4 eight node elements is used in a quadrant of the shell. The problem is linearly analyzed. The vertical displacement at the middle of the free edge is computed. Figure (6.8) and (6.9) shows the variation of the vertical deflections at the middle of the free edge and horizontal

displacement at rigid support respectively, while Figure (6.10) shows the convergence of the vertical displacement.

The results obtained are in close agreement with those reported by Simo, Fox and Rifai [37].

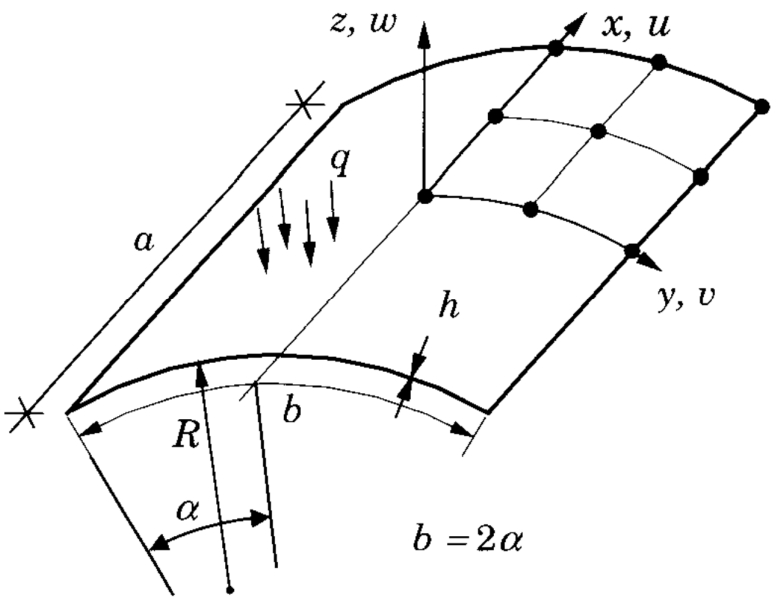


Figure (6.7) cylindrical shell roof under its own weight

The barrel vault problem is also analyzed when the shell is laminated of a composite material. The data of the problem is α=40 R=300 in., a=600 in. and

$E_1=25E_2$, $E_2=1$, $G_{12}=G_{13}=0.5E_2$, $G_{23}=0.2E_2$, $\nu_{12}=0.25$,

A quadrant of the panel is modeled with 4x4 eight node mesh. The following dimensionless quantities are presented in Table (6. 1).

$$w = 10\, w_B \frac{E_1 h^3}{qR^4}$$

Table (6.3) contains the nondimensionalized deflection for two-layer and ten –layer antisymmetric cross-ply (0/90/0/90/……)laminated shells for different radius- to- thickness ratio, s=R/h.

Results obtained are in good agreement with those obtained by J. N. Reddy [ 6 ].

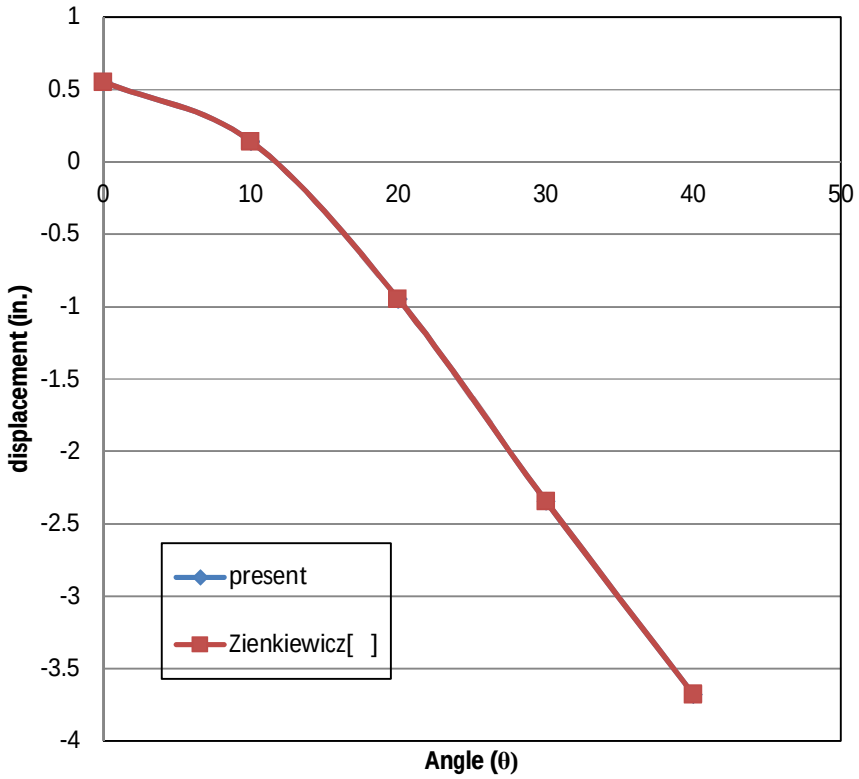


**Figure( 6.8) Vert**ical deflection at centre of free edge

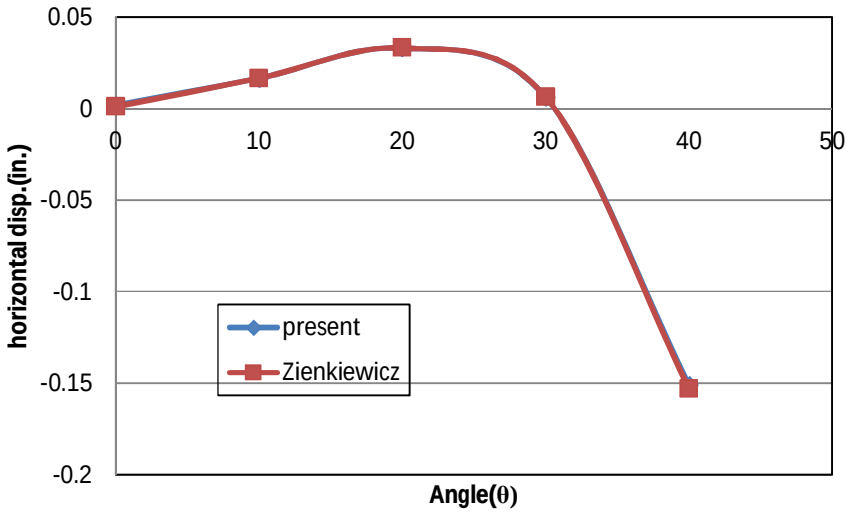


Figure (6.9) Horizontal displacement

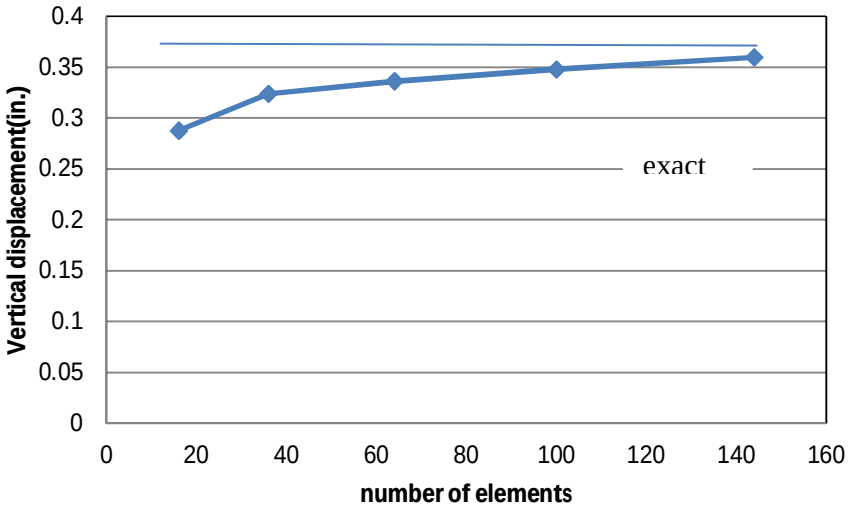


Figure ( 6.10) Convergence of vertical deflection
(exact solution reported by Simo.Fox and Rifai [ 34 ] as w=-3.6288 in. )

Table (6.5) Maximum transverse deflections of cross-ply laminated cylin derical shell roof under its own weight

| Layers | S=R/h | Present | Ref.[ 34] | Diff.(%) |
|---|---|---|---|---|
| 2 | 20 | 12.6309 | 12.1529 | 4% |
| | 50 | 5.4694 | 5.4211 | 0.89% |
| | 100 | 3.0869 | 3.1191 | 1.03% |
| 10 | 20 | 8.8349 | 8.7239 | 1.27% |
| | 50 | 3.0856 | 3.1358 | 1.61% |
| | 100 | 1.8542 | 1.8877 | 1.77% |

### 6.1.5 Pinched cylinder:

This is another well-known benchmark problem. The circular cylinder with rigid end diaphram is subjected to a point load at the centre on opposite sides of the cylinder , as shown in Figure (6.11). The geometric and material data of the problem is

$\alpha=\pi/2$ rad. $R=300$ in. $a=600$ in. $h=3$ in. $E=3\times10^6$ psi $\nu=0.3$

The boundary conditions used are:

At $x=0$: $u=\beta=0$ , at $x=a/2$: $v=\alpha=w=0$, at $y=0,b/2$ : $v=\alpha=0$

One octant of the cylinder was modelled with 8×8 eight node and linearly analysed using **NFEAP** and the vertical displacement computed is $1.7191\times10^{-5}$ in. The displacements are presented in Table(6.6). The analytical solution of Flugge [17] is $-1.8248\times x10^{-5}$ in, Cho and Roh [36] reported the value of $-1.8541\times10^{-5}$ in. It is clear that solution can be improved by increasing number of elements in the mesh considered.

Table (6.6) Displacements at point (A) of the laminated pinched circular cylinder problem.

| Layers | S=R/h | Ref. [17] | Present | Diff.(%) |
|---|---|---|---|---|
| 2 | 100 | 1.2450 | 1.2893 | 3.4% |
| 2 | 50 | 2.3756 | 2.0713 | 14% |
| 2 | 20 | 6.0742 | 4.4759 | 26% |

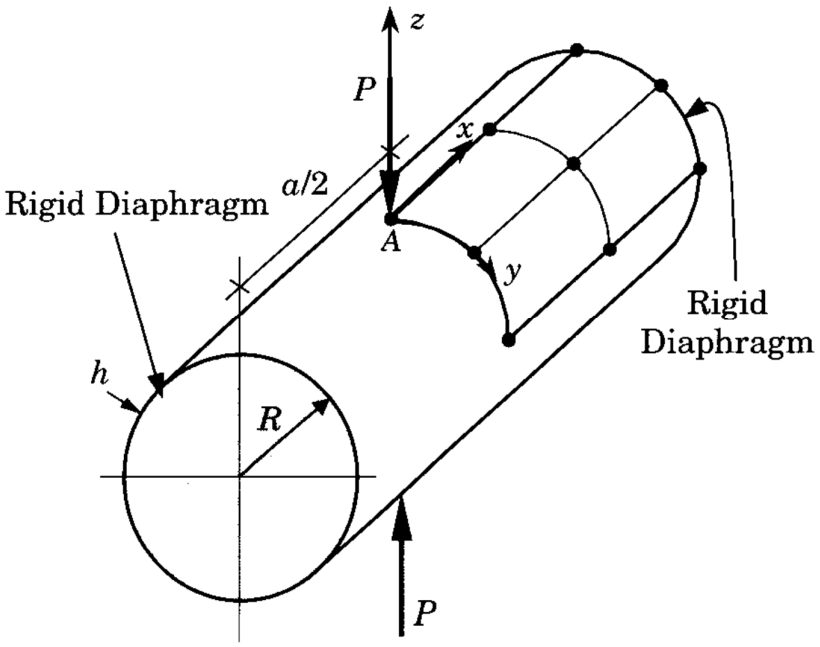


Figure (6.11) Pinched cylindrical shell

6- **Laminated cylindrical shell:**

This example involves the laminated cylindrical shell shown in Figure (6.12). The geometry appears in various articles but the current example was adapted from To and Liu [27] who developed an enhanced full layer wise 3-node triangular element for geometrically non-linear analysis.

The cylindrical shell is hinged at straight sides and free at the two curved ends. The entire geometry is modeled with side length L=508 mm, radius of curvature R=2540 mm and angle 2θ=0.2 radians. The lay-up is an antisymmetric +45/-45 (measured from the global x-axis) laminate of equal thickness layers and a total thickness of $h$=12.4 mm. The material properties are stated in the material coordinate system (1-axis aligned with the global x-axis) as $E_1=3.2993\times10^6$ MPa, $E_2=E_3=1.0998\times10^6$ MPa, $G_{12}=G_{13}=4.4128\times10^5$ MPa, and $\nu=0.25$. One quadrant of the panel is modeled with 4x4 eight node elements and nonlinearly analyzed using **NFEAP**. The results from the current element formulation are presented

in Figure (6.13) and compared to the results obtained with a 8x8 mesh of triangular elements by To and Liu [27]. Good correlation between data obtained was observed. Table (6.7) shows the vertical displacements of the apex of the cylindrical panel. The two formulations yield approximately the same results.

Table (6.8) compares the moments (Mx) at the centre of the shell while Table (6.8) compares the resultant forces (Nx) at the centre of the supported side of the shell. The results obtained using the two formulations are approximately the same.

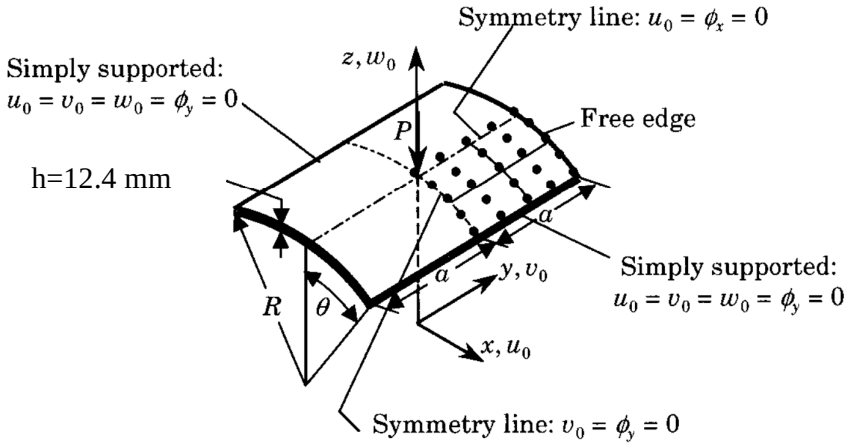


Figure (6.12) Cylindrical laminated shells

Table (6.7) Vertical displacement (mm) vs. load (kN)

| load factor | Ref.[27 ] | Green strains | Geometric strains |
|---|---|---|---|
| 0 | 0 | 0 | 0 |
| 0.2 | 1 | 0.9725 | 0.9723 |
| 0.4 | 2 | 2.0614 | 2.0604 |
| 0.6 | 3.5 | 3.3156 | 3.3134 |

| | | | |
|---|---|---|---|
| 0.8 | 4.7 | 4.8545 | 4.8282 |

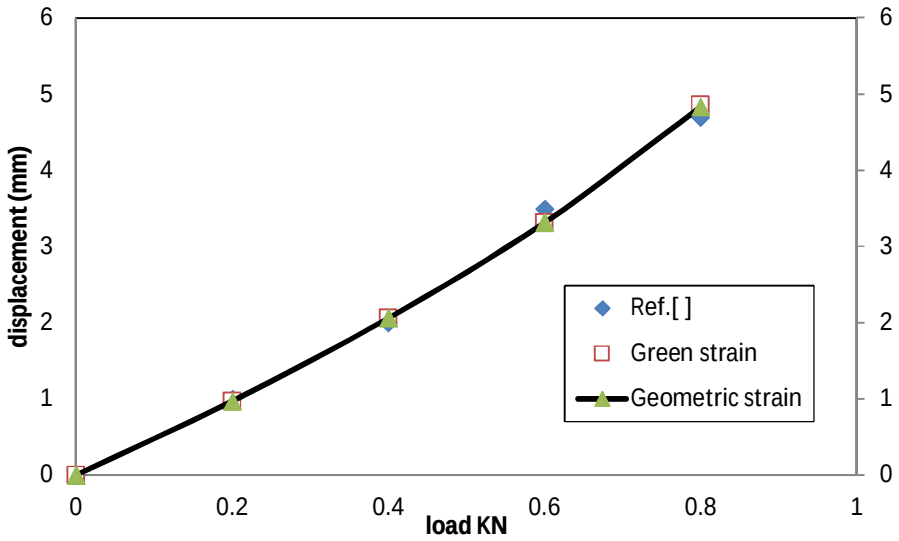


Figure(6.13) Results of non-linear analysis of cylinderical laminated shell

Table (6.8) Comparison of moments ($10^3 \times M_X$) at the centre of the shell

| Incr. No. | Load Kn | Green moments N-m/m | Geom. Moments N-m/m | Difference percent (%) |
|---|---|---|---|---|
| 1 | 0.05 | 0.037 | 0.037 | 0.00 |
| 2 | 0.10 | 0.079 | 0.079 | 0.00 |
| 3 | 0.15 | 0.125 | 0.125 | 0.70 |

| | | | | |
|---|---|---|---|---|
| 4 | 0.20 | 0.177 | 0.176 | 0.60 |
| 5 | 0.25 | 0.236 | 0.235 | 0.40 |
| 6 | 0.30 | 0.305 | 0.303 | 0.70 |
| 7 | 0.35 | 0.387 | 0.385 | 0.50 |
| 8 | 0.40 | 0.490 | 0.485 | 1.02 |
| 9 | 0.45 | 0.628 | 0.617 | 1.80 |
| 10 | 0.50 | 0.844 | 0.816 | 3.30 |

Table (6.9) Comparison of resultant forces ($10^3$ x Nx) at the centre of the supported(hinged) side shell

| Incr. No. | Load KN | Green moments N-m/m | Geom. Moments N-m/m | Difference percent (%) |
|---|---|---|---|---|
| 1 | .05 | .046 | .046 | 0 |
| 2 | .10 | .091 | .091 | 0 |
| 3 | .15 | .136 | .136 | 0 |
| 4 | .2 | .180 | .180 | 0 |
| 5 | .25 | .223 | .224 | .4 |
| 6 | .30 | .266 | .268 | .8 |
| 7 | .35 | .309 | .311 | .6 |
| 8 | .40 | .351 | .354 | .9 |
| 9 | .45 | .393 | .398 | 1.3 |
| 10 | .50 | .437 | .445 | 1.8 |

### 6.1.7 Doubly curved shell panel:

Next, we consider a spherical shell panel ($R_1=R_2=R$) under central point load. The shell panel is simply supported at all edges as shown in Figure (6.14). The geometric and material parameters used are:

R=96 in. a=b=32 in. h=0.1 in.

$E_1=25E_2$, $E_2=1E6$ psi, $G_{12}=G_{13}=0.5E_2$, $G_{23}=0.2E_2$, $v_{12}=0.25$

The point load is taken to be $F_0=100$ lbs. The numerical results obtained using a mesh of 4x4 eight node elements in a quadrant of the shell are presented in Table(6.10), Good agreement between results obtained and that published in Ref.[33] can be observed.

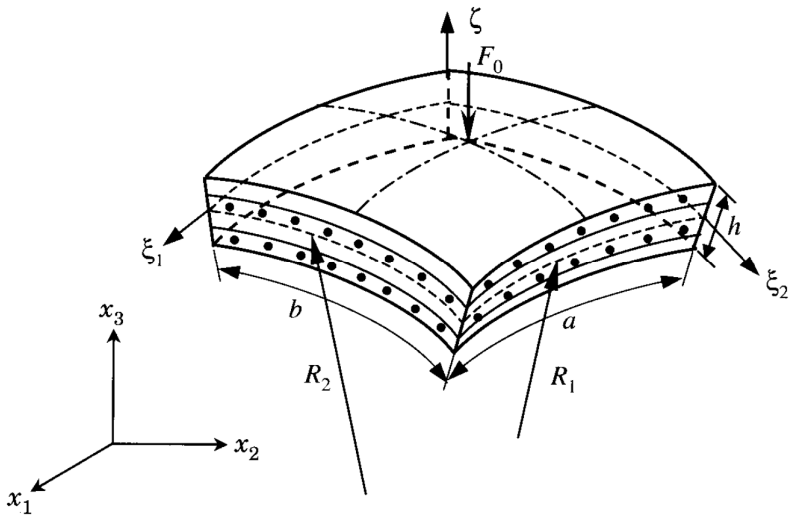


Figure (6.14) simply supported spherical shell panel under central point load

Table (6.10) Maximum radial deflection (-w×10 in.) of a simply supported spherical shell panel under central point load.

| Laminate | Present | Ref. [33] | Diff.(%) |
|---|---|---|---|
| Orthotropic | 0.9596 | 1.0340 | 7.1% |
| 0/90 | 0.9553 | 1.0217 | 6.5% |

| | | | |
|---|---|---|---|
| 45/-45 | 0.5504 | 0.6051 | 9.0% |

## 6.2 DICUSSION OF RESULTS

In this research computer program coded in **FORTRAN 77** is developed for the analysis of geometrically nonlinear finite element laminated shell structures. Eight nodes degenerated finite element is used as a basic element for the finite element formulation. The formulation adopts Total Lagrangian formulation using both Green's strain and Geometric strain.

The nonlinear equilibrium equations are solved incrementally and iteratively adopting incremental process coupled with Newton-Raphson Method.

In order to assess the performance of the formulation, seven laminated shell structures are analyzed using the developed formulation including cylindrical shell, spherical shells and flat plates. Here in after is the discussion of obtained results:

**In Example (6.1.1)** a simply supported square plate under uniform distributed load was analyzed. Rapid convergence of central deflection was observed even with coarse mesh. Here a question can be asked stating like this (what is the optimum number of finite elements are required for proper analysis?). More elements may lead to inaccurate results and expensive solution.

**In example (6.1.2)** an orthotropic plate subjected tom uniformly distributed load and simply supported is linearly and nonlinearly was analyzed. Vertical displacements obtained using Green's strain and Geometric strain is approximately the same and compare very well with results of Ref. [9]. The same data are presented in Table (6.5) confirm the above conclusion.

**In Example (6.1.3),** a square laminated plate (0/90/90/0) is simply supported under sinusoidal load analyzed for deflections and stresses. The results obtained are in good agreement when compared with the analytical solution Ref. [7].

The mathematical model proposed for predicting deflections in terms of modulus ratios $E1/E_2$ perform very well as shown in the graph in Figure (6.5) and Table (6.4).

Figure (6.6) conclude that deflections converge to FSDT (First Order Shear Deformation Theory) when side–to–thickness ratio reaches (100). CPT (Classical Plate Theory) is not affected by thickness.

**In Example (6.1.4)**, barrel vault under its own weight is linearly analyzed. This is a well known bench mark problem used by many authors for comparison. The vertical displacement of the centre of the free side is plotted for convergence. It observed that there is a rapid convergence even with coarse mesh see Figure (6.8). Figures (6.5) and (6.5) show the variation of vertical and horizontal displacements with respect to the central angle. Good agreement was observed with data presented in Ref. [34].

The same barrel analyzed as laminated shell structures. Table (6.6) presents the displacements obtained and the difference between reference values and present values. Small differences are found'.

**In Example (6.1.5)** pinched cylindrical shell shown in Figure (7.7) is linearly analyzed. This is another well-known benchmark problem. The circular cylinder with rigid end diaphram is subjected to a point load at

the centre on opposite sides of the cylinder , as shown in Figure 6.5. The displacent at point (A) is evaluated and compared with that found in ref.[6]. Some large differences was observed. It need to invesigate the reasons for this large differences.

**In Example (6.1.6)** a hinged cylinderical two layer shell is analysed nonlinearly.

The central displacents obtained using Green's strain and Geometric strain are tabulated in Table (6,.8 ) for comparisons. Both results are in good agreement with results of Ref.[8]. To obtain a full path for this snap-through problem the solution method should be modified by using Arc-Length method in order to pass the limit points.

**In the last Example (6.1.7)**a spherical shell subjected to concentrated load. Orthotropic, angle ply and cross ply scheme are formed. The displacement under the load is evaluted . Good agreement between results obtained and that published in Ref. [21] can be observed.

# CHAPTER SEVEN
# CONCLUSIONS AND RECOMMENDATIONS

## 7.1 Conclusions:

In this research computer program coded in FORTRAN 77 is developed for the analysis of geometrically nonlinear finite element laminated shell structures. Eight nodes degenerated finite element is used as a basic element for the finite element formulation. The formulation adopts Total Lagrangian formulation using both Green's strain and Geometric strain.

The nonlinear equilibrium equations are solved incrementally and iteratively adopting incremental process coupled with Newton-Raphson Method. The results obtained from analysis of different structure configuration are compared with known published results and hence the following conclusions are drawn:

1. The degenerated eight node shell finite element shows good performance when used to analyze laminated shell structures. This is confirmed when comparing results obtained with analytical known solutions.
2. Results obtained using Green's strain are approximately the same as that obtained when using Geometric strain for both curved shells and flat shells (plates)
3. The proposed mathematical model for predicting deflections in terms of modular ratios compare very well with finite element solutions
4. No shear locking is observed when using reduced integration with eight Gauss point

5. Displacement and stresses obtained for plates are more accurate than that of shell , this may be due to the transformation of the constitutive equations , stresses and strains
6. Percent difference for displacements are less than that for stresses for the same increment, the reason is that displacements are directly computed at Gauss points but stresses are derived from displacement , hence approximation is increased.

## 7.2 Recommendations for further studies:

The following recommendations may be considered for future studies:

1. The modification of the program to include material nonlinearity.
2. Extending the program to solve dynamic practical problems.
3. Incorporate Arc-Length Method to obtain full displacement path by passing limit points encountered during using Newton Raphson Method in solving non-linear equations.
4. Develop smart interface for **NFEAP** using Visual Basic
5. More cases can be formulated by altering loads, boundary conditions and mesh type.

**References:**

[1] Ochoa O. O. and Reddy J. N., "Finite element analysis of composite laminates", Kluwer Academic Publisher, 1992.

[2] Reddy J. N., "A review of refined theories of laminated composite plates", Shock Vib. Dig., Vol. 22 , pp., 3-7, 1990.

[3] Reddy J. N., "On refined computational models of composite laminates", International journal for numerical methods for engineering, Vol. 27, pp.361-382, 1989.

[4] Reddy J. N., "A Simple higher–order theory for laminated composite plates", Journal of Applied Mechanics, ASME 51, 1984.

[5] Reddy J. N., "A generalization of 2-dimensional theories of laminated Plates", Comm. Applied for numerical methods, Vol. 3, pp. 173-180, 1987.

[6] Bathe K. J., "Finite element procedures", 2nd edition, Prentice-Hall Inc., 1996.

[7] Belegundu A. D. and Chandrupatla T. R., "Introduction to finite elements in engineering", 3rd edition, Printice - Hall, 2002.

[8] Krishnamoorthy C. S. ,"Finite Element Analysis–theory and programming", 2nd edition, Tata McGraw - Hill, 1994.

[9] Crisfield M. A., "Non-linear finite elements analysis of solids and structures", Volume 1, John Wiley & Sons Ltd., 1991.

[10] Crisfield M. A., "Non-linear finite elements analysis of solids and structures", Volume 2, John Wiley & Sons Ltd., 1997.

[11] Reddy J. N., "Mechanics of laminated plates and shells-theory and analysis", 2nd edition, CRC press LLC, 2004.

[12] Reddy J. N., "An Introduction to the fnite element method", 2nd edition, McGraw - Hill Inc., 1984.

[13] Timoshenko S. P. and Goodier J. N., "Theory of elasticity", 2nd edition, McGraw - Hill Inc., 1951.

[14] Timoshenko S. P. and Krieger S. W., “Theory of plates and shells”, 2nd edition, McGraw - Hill Inc., 1959.

[15] Zienkiewicz O. C. and Taylor R. L., “The finite element method–basic formulation and linear problems”, Volume 1, McGraw - Hill Inc., 1989.

[16] Zienkiewicz O. C. and Taylor R. L., “The finite element method - solid mechanics”, Volume 2, 5th edition, McGraw - Hill Inc., 2000.

[17] Stegmann Jan “Analysis and optimization of laminated composite shell structures”, Ph. D. Thesis, Institute of Mechanical Engineering - Aalborg University, 2005.

[18] Adam F. M., “Linear and non-linear fnite element analysis of large deformation of thin shell structures”, Ph.D. Thesis, Sudan University of Science and Technology, 2008.

[19] Mohamed A. E., “A Small strain large rotation theory and finite element formulation of thin curved beams”, Ph.D. Thesis, The City University, 1983.

[20] Dvorkin E. N. and K. J. Bathe “A Continuum mechanics based four-node shell element for general nonlinear analysis”, Journal of Engineering Computations 1,77–88,1984.

[21] Kumar W.P. and Palaninathan R., “Finite element analysis of laminated shells with exact through-thickness integration”, Computers & Structures,63, pp.173–180, 1997.

[22] Lund E. and T. J. Condra, “Notes and exercises for course on numerical methods”, Lecture notes available at www.ime.auc.dk/.el.,2001.

[23] Stegmann J., L. R. Jensen and J. M. Rauhe “Finite elements for geometric non-linear analysis of composite laminates and sandwich

structures” M. Sc. Thesis, Institute of Mechanical Engineering - Aalborg University, 2001.

[24] Bucalem M. L. and Bathe K. J. , “Higher-order MITC General Shell Elements”, International Journal for Numerical Methods in Engineering 36, pp 3729 -3754, 1993.

[25] Jones R. M., “Mechanics of Composite Materials”, 2nd edition, Taylor & Francis, 1999.

[26] Zaghloul S. A. and Kenedy, J. B., “Nonlinear analysis of unsymmetrical laminated plates”, Journal of Applied Mechanics, 42, pp. 234-236, 1975.

[27] To C. W. S. and Liu M. L., “Geometrically nonlinear analysis of layerwise anisotropic shell structures by hybrid strain based lower order Elements”, Finite Element s in Analysis and Design, Vol. 37, pp. 1-34, 2001.

[28] Dvorkin E. N. and Bathe K. J. “A Continuum mechanics based four node shell element for general nonlinear analysis”, Engineering Computer, Vol. 1,1984.

[29] Balah M. and Al-Ghamedy H. N., “Finite element formulation of a third order laminated finite rotation shell element”, Computer and Structures, Vol. 80, pp. 1975-1990, 2002.

[30] Alfano G. *et al*, “MITC finite elements for laminated composite plates”, International journal for numerical methods in engineering, Vol. 50, pp. 707-738, 2001.

[31] Mohan P., “Development and application of a flat triangular element for thin laminated shells”, Ph.D. Thesis, Ph.D. Thesis, Virginia Polytechnic Institute, 1997.

[32] Rao K. P., “A Rectangular laminated anisotropic shallow shell finite element”, Computer Methods in Applied Mechanics and Engineering, 15, pp. 13-33, 1978.

[33] Vlasov V. Z., “General theory of shells and its applications in engineering”, NASA TT RF-99, National Aeronautics Administration, Washington, D.C. (1964).

[34] Cantin G. and Clough R. W., “A Curved cylindrical shell finite element”, AIAA Journal, Vol. 6, pp. 10-57, 1968.

[35] Flügge W. Stresses in shells, 2nd edition, Springer-Verlag, Berlin, Germany, 1973.

[36] Cho M. and Roh H. Y., “Development of geometrically exact element based on general curvilinear coordinates, International Journal for Numerical Methods in Engineering”, Vol. 56, pp. 81-115, 2003.

[37] Simo J. C., Fox D. D. and Rifai M. S., “On stress resultant geometrically exact shell model. Part II: The Linear Theory, Computer Methods in Applied Mechanics and Engineering, Vol. 73, pp. 53-92, 1989.

[38] Ahmad S., Irons B. M. and Zienkiewicz O. C., "Analysis of Thick Shell and Thin Shell Structures by Curved Finite Elements", International Journal for Numerical Methods in Engineering 2, pp. 419 - 459, 1970.

[39] To C. W. S. and Wang B., “Hybrid strain based geometrically nonlinear laminated composite triangular shell finite elements”, Finite Elements in Analysis and Design, Vol. 33, pp. 83-124, 1999.

[40] Klinkel S. *et al*, “A Continuum based 3D shell element for laminated structures” , Institute of Balstork, 12, D-76131, Karlsruhe

[41] Masud A. and Panahandeh M., “A Finite element formulation of multi-layered Shells for the analysis of laminated composites”, Computer and Structures, Vol. 148, 1980.